



Redescription of the holotype specimen of *Chindesaurus bryansmalli* Long and Murry, 1995 (Dinosauria, Theropoda), from Petrified Forest National Park, Arizona

Adam D. Marsh, William G. Parker, Max C. Langer & Sterling J. Nesbitt

To cite this article: Adam D. Marsh, William G. Parker, Max C. Langer & Sterling J. Nesbitt (2019): Redescription of the holotype specimen of *Chindesaurus bryansmalli* Long and Murry, 1995 (Dinosauria, Theropoda), from Petrified Forest National Park, Arizona, Journal of Vertebrate Paleontology

To link to this article: <https://doi.org/10.1080/02724634.2019.1645682>

 View supplementary material 

 Published online: 04 Sep 2019.

 Submit your article to this journal 

 View related articles 

 View Crossmark data 

REDESCRIPTION OF THE HOLOTYPE SPECIMEN OF *CHINDESAURUS BRYANSMALLI* LONG AND MURRY, 1995 (DINOSAURIA, THEROPODA), FROM PETRIFIED FOREST NATIONAL PARK, ARIZONA

ADAM D. MARSH, ^{*1,2} WILLIAM G. PARKER, ² MAX C. LANGER, ³ and STERLING J. NESBITT ⁴
¹Jackson School of Geosciences, The University of Texas at Austin, Austin, Texas 78705, U.S.A., adam_marshall@nps.gov;

²Division of Resource Management, Petrified Forest National Park, Petrified Forest, Arizona 86028, U.S.A., william_parker@nps.gov;

³Laboratório de Paleontologia, Faculdade de Filosofia, Ciências e Letras de Ribeirão Preto, Universidade de São Paulo, Ribeirão Preto, Sao Paulo 14040-220, Brazil, mclanger@ffclrp.usp.br;

⁴Department of Geosciences, Virginia Polytechnic Institute and State University, Blacksburg, Virginia 24061, U.S.A., snj2104@vt.edu

ABSTRACT—*Chindesaurus bryansmalli* is an early dinosaur of uncertain affinities from the Late Triassic Chinle Formation at Petrified Forest National Park, Arizona. Since its first description in 1995, the taxon has been considered a plateosaurid, a non-eusaurischian saurischian, a herrerasaurid, and/or a non-neotheropod member of Theropoda. *Chindesaurus bryansmalli* is usually scored for about 25% of the characters in a given phylogenetic analysis, and many characters have been scored secondhand from misidentified elements. Here, we provide a redescription of the holotype specimen of *C. bryansmalli*, correct misidentifications, introduce previously unknown elements, and discuss novel morphological character observations. *Chindesaurus bryansmalli* is supported as the sister taxon to the non-neotheropod theropod *Tawa hallae* from the Chinle Formation at Ghost Ranch, New Mexico. The same two most parsimonious trees, with increasing node support, result from iteratively removing the three most incomplete taxa in the employed data set, suggesting that the relationships of stem-averostran theropods are not highly affected by the inclusion of fragmentary specimens. The *Chindesaurus* + *Tawa* clade recovered here may represent a potentially diverse group of early theropods prior to the end-Triassic mass extinction.

SUPPLEMENTAL DATA—Supplemental materials are available for this article for free at www.tandfonline.com/UJVP

Citation for this article: Marsh, A. D., W. G. Parker, M. C. Langer, and S. J. Nesbitt. 2019. Redescription of the holotype specimen of *Chindesaurus bryansmalli* Long and Murry, 1995 (Dinosauria, Theropoda), from Petrified Forest National Park, Arizona. *Journal of Vertebrate Paleontology*. DOI: 10.1080/02724634.2019.1645682.

INTRODUCTION

The holotype specimen of *Chindesaurus bryansmalli* was discovered in 1984 at Petrified Forest National Park, Arizona, by Bryan Small, who first found an astragalus that immediately identified the specimen as what was at the time thought to be the oldest known dinosaur. The skeleton was excavated by a field crew led by Robert Long, then from the University of California Museum of Paleontology (UCMP). On June 6, 1985, the holotype of *C. bryansmalli*, or ‘Gertie’ (named after the first-ever animation of a dinosaur in 1914), was airlifted by a Sikorsky helicopter from the Painted Desert area of the park (Robert Long field notes, 1984:308–310, 1985:332–333; Miller, 1985; Dunbar and Robson, 1986; Meyer, 1986). After being prepared at the UCMP, it was realized that this specimen represented not a plateosaurid as originally announced in a news conference from the field (Padian, 1988) but was probably an early theropod dinosaur (Long and Murry, 1995).

When *Chindesaurus bryansmalli* was named, it was thought to represent a ‘staurikosaurid dinosaur’ (Murry and Long, 1989) or ‘herrerasaurid dinosauriform’ (Long and Murry, 1995:173). Citing the presence of anteroposteriorly short dorsal vertebrae, two sacral vertebrae, and a narrow pubic apron, Novas (1997) agreed that *C. bryansmalli* was a herrerasaurid. Later, Rauhut (2003) considered the taxon a nomen dubium without further

comment, but Langer (2004) considered it a saurischian dinosaur outside of Eusaurischia (Langer et al., 2009). *Chindesaurus bryansmalli* is rather ubiquitous in numerous phylogenetic analyses of dinosauriforms (Irmis et al., 2007), early dinosaurs (Baron et al., 2017a, 2017b; Langer et al., 2017; Baron and Williams, 2018), ornithischians (Baron and Barrett, 2017), sauropodomorphs (Yates, 2007, and derivative matrices), and theropods (Nesbitt et al., 2009c; Ezcurra and Brusatte, 2011; Sues et al., 2011; Nesbitt and Ezcurra, 2015), but its phylogenetic affinities remain debated.

One of the first phylogenetic analyses to use *Chindesaurus bryansmalli* as an operational taxonomic unit was Irmis et al. (2007), recovering the taxon within Herrerasauridae, but outside Theropoda (see also Sues et al., 2011). *Chindesaurus bryansmalli* was also recovered as a herrerasaurid when that clade was recovered in a basal polytomy with other early theropods (Ezcurra and Brusatte, 2011) or as a group of non-neotheropod theropods (Nesbitt et al., 2009c). The first analysis to suggest that *C. bryansmalli* was not a herrerasaurid hypothesized it to be a non-neotheropod member of Theropoda (Yates, 2007; Nesbitt and Ezcurra, 2015; Langer et al., 2017). Recent phylogenetic hypotheses of early dinosaur relations recover *Chindesaurus bryansmalli* either as a non-theropod herrerasaurid within a newly redefined Saurischia (Baron et al., 2017a), immediately outside Ornithoscelida (Baron and Barrett, 2017; Baron et al., 2017b), or as a herrerasaurid dinosauriform (Baron and Williams, 2018). A recent hypothesis redefined Saurischia (the most inclusive clade containing *Diplodocus carnegii* but not

*Corresponding author.

Triceratops horridus; Baron et al., 2017a), but we refer to Saurischia using the traditional definition (the most inclusive clade containing *Passer domesticus* but not *Triceratops horridus*; Sereno, 2005) owing to the lack of compelling support for the ‘Ornithoscelida’ hypothesis (Langer et al., 2017).

Having been positioned either as the outgroup or an early diverging member of a variety of major dinosaur groups, *Chindesaurus bryansmalli* has been an important taxon in the optimization of character states in phylogenetic analyses of early dinosaurs. Because it was first named in the absence of a phylogenetic analysis (Long and Murry, 1995), *C. bryansmalli* has yet to be formally diagnosed by apomorphies in its own phylogenetic context. Additionally, many published character scores for *C. bryansmalli* have not changed much between analyses (with the exception of Langer et al., 2017), suggesting that many of the scores are based on the literature. Finally, some of the original identifications of bones that have been propagated in the literature are incorrect, with obvious effects on phylogenetic analyses that use *C. bryansmalli* as an operational taxonomic unit.

The unifying theme of the uncertain evolutionary relationships of *C. bryansmalli* is the missing data inherent to each analysis that includes it as a terminal taxon. Many characters that are important to the early evolution of dinosauriforms are found in the pelvis and hind limb (e.g., Sereno, 1999; Langer and Benton, 2006; Nesbitt et al., 2007; Baron et al., 2017a), and even though the holotype of *C. bryansmalli* preserves some of those regions, its fragmentary nature leaves phylogenetic hypotheses poorly supported. At best, *C. bryansmalli* has been scored for ca. 25% of the characters in prior phylogenetic analyses (Table 1). Yet, many dinosauriform taxa are even less complete than *C. bryansmalli* and some are represented by a single element (i.e., *Camposaurus*) or a small number of elements (i.e., *Dromomeron gregorii*, *Eucoelophysis baldwini*, and *Lepidus praecisio*).

Here, we redescribe the holotype of *Chindesaurus bryansmalli*, correcting the previously misidentified elements, and provide a new phylogenetic context for this important Late Triassic North American dinosaur. In addition, we present sensitivity analyses performed by iteratively removing incomplete taxa from a revised and updated character-taxon matrix of Mesozoic archosaurs in order to investigate the effect of missing data on this particular branch of the archosaur tree.

Institutional Abbreviations—**GR**, Ruth Hall Museum of Paleontology at Ghost Ranch, Abiquiu, New Mexico, U.S.A.; **NMMNH**, New Mexico Museum of Natural History and Science, Albuquerque, New Mexico, U.S.A.; **PEFO**, Petrified Forest National Park, Arizona, U.S.A.; **TMM**, Texas Memorial

Museum collections at the Vertebrate Paleontology Laboratory, Austin, Texas, U.S.A.; **TTU**, Museum of Texas Tech University, Lubbock, Texas, U.S.A.; **UCMP**, University of California Museum of Paleontology, Berkeley, California, U.S.A.; **UMMP**, University of Michigan Museum of Paleontology, Ann Arbor, Michigan, U.S.A.

Other Abbreviations—**MOTT**, refers to a locality number from TTU-P; **PFV**, refers to a locality number from PEFO.

SYSTEMATIC PALEONTOLOGY

DINOSAURIA Owen, 1842, sensu Sereno, 2005
SAURISCHIA Seeley, 1887, sensu Sereno, 2005
THEROPODA Marsh, 1881, sensu Sereno, 2005

CHINDESAURUS BRYANSMALLI Long and Murry, 1995

Holotype Specimen—PEFO 10395, partial skeleton including cervical and dorsal centra, sacral and caudal vertebrae, hemal arches, right and left pubic peduncles of the ilia, partial iliac blade and left postacetabular process of the ilium, partial pubes, proximal end of left femur, complete right femur, partial right tibia, and partial right astragalus. The holotype specimen was listed incorrectly as PEFO 33982 in two studies (Stocker, 2013; Langer et al., 2017). One nearly complete anterior caudal vertebra was figured by Long and Murry (1995:figs. 177d–h and 179a–e) as a dorsal vertebra but was later separated at the UCMP from the rest of the holotype material (Fig. 3A–F). We relocated the vertebra while visiting the UCMP, which included a written note saying that it was not from the holotype. Because no indication is given in the field notes of the excavation of the holotype that the vertebra is not associated with the rest of the specimen, we retain this vertebra in the holotype specimen. Three-dimensional surface files of PEFO 10395 are available in MorphoBank (MorphoBank P3384). More than one individual was thought to be in the block containing the holotype, including a smaller partial pelvis and hind limb. These probably belong to a shuvosaurid, but those bones have been missing since the preparation of the block (T. Rowe, pers. comm., 2017; Rob Long field notes, 1985; Dunbar and Robson, 1986; Long and Murry, 1995; Parker, 2006).

The skeletal maturity of the holotype specimen at the time of death is unknown, and to date no histological study (e.g., Padian, 2013; Woodward et al., 2013) has been performed to estimate this. Along with the incorporation of more vertebrae into the sacrum (Rauhut, 2003; Tykoski, 2005), the co-ossification of certain skeletal elements has often been used to indicate

TABLE 1. Description of various character-taxon matrices for which *Chindesaurus* has been included, including the phylogenetic position of the taxon as an outcome of that analysis.

Study	Number of taxa in analysis	Number of characters in analysis	Scoring completeness for <i>Chindesaurus</i>	Phylogenetic position of <i>Chindesaurus</i>
Irmis et al., 2007	26	127	25.98%	Herrerasaurid, outside of Theropoda
Nesbitt et al., 2009a	41	315	20.32%	Herrerasaurid, outside Neotheropoda
Sues et al., 2011	42	319	20.06%	Herrerasaurid, outside Theropoda
Ezcurra and Bruschate, 2011	43	339	21.53%	Herrerasaurid in basal polytomy
Nesbitt and Ezcurra, 2015	45	343	22.16%	Non-neotheropod
Baron et al., 2017a	74	457	14.66%	Herrerasaurid, basal saurischian
Langer et al., 2017	74	457	15.10%	Non-neotheropod
Baron et al., 2017b	74	457	14.66%	Non-ornithischelidan saurischian
This study	45	352	25.00%	Non-neotheropod

skeletal maturity in archosaurs, including that of the centra with the respective neural arches (Brochu, 1996; Irmis, 2007) and distal ends of the tibia and the fibula with the proximal tarsals (Rowe, 1989; Colbert, 1990; Tykoski, 1998, 2005). Although these co-ossifications and the development of muscle scars vary significantly along the ontogeny of some dinosauriform lineages (Griffin and Nesbitt, 2016a, 2016b; Griffin, 2018), and thus might not be reliable indicators of skeletal maturity for theropods, it is worth mentioning that the holotype of *Chindesaurus bryansmalli* preserves presacral centra isolated from the neural arches, whereas those of the tail are co-ossified, and that the distal end of the tibia is not co-ossified to the astragalus. The holotype femur of *Chindesaurus bryansmalli* has a trochanteric shelf integrated into the anterior trochanter, but other referred specimens (see below) do not. The paucity of skeletons of this taxon makes it difficult to estimate its ontogenetic variability (Evans et al., 2018).

Referred Specimens—Only the holotype specimen is complete enough to preserve the unique combination of character states that diagnose the taxon (see Discussion).

Removed Specimens—The following specimens previously have been referred to *Chindesaurus bryansmalli* but are either lost or are not complete enough to preserve the unique combination of character states of the taxon as outlined in the revised diagnosis below (but they potentially belong to the *Chindesaurus bryansmalli* + *Tawa hallae* clade hypothesized below): PEFO 33982, dorsal and sacral vertebrae, proximal end of left femur (Parker and Irmis, 2005; Nesbitt et al., 2007); PEFO 4849, dorsal centrum (Long and Murry, 1995); PEFO 34875, proximal end of right femur; PEFO 36766, dorsal centrum; PEFO 34583, proximal end of left femur; PEFO 36730, dorsal centrum, caudal vertebrae; PEFO 40754, proximal end of right femur; PEFO 34605, distal end of right femur, fragmentary left femur; NMMNH P-4415, proximal end of left femur (Long and Murry, 1995:174; Heckert et al., 2000); NMMNH P-16656, dorsal and caudal vertebrae (Long and Murry, 1995; Heckert et al., 2000; Nesbitt et al., 2007); NMMNH P-17325, dorsal centrum (Long and Murry, 1995; Heckert et al., 2000); NMMNH P-35996, partial left ilium; UMMP 8870, left ilium (Long and Murry, 1995; *Caseosaurus crosbyensis*, Case, 1927:220; Hunt et al., 1998; Nesbitt et al., 2007); NMMNH P-35995, dorsal and sacral vertebrae, partial right ilium, proximal end of left femur (cf. *Caseosaurus crosbyensis*; Nesbitt et al., 2007; Baron and Williams, 2018); NMMNH P-52860, distal end of left femur; five dorsal centra and two co-ossified sacral vertebrae (missing, UCMP number unknown; Long and Murry, 1995); UCMP 25789, distal end of right femur; TMM 31100-523, proximal end of left femur (Long and Murry, 1995; Nesbitt et al., 2007; Stocker, 2013); and GR 226, complete right femur.

An apomorphy-based identification of the holotype of *Caseosaurus crosbyensis* (UMMP 8870) limited its identification to Dinosauriformes (Nesbitt et al., 2007) and determined that name to be a nomen dubium. A recent redescription of the holotype found *Caseosaurus crosbyensis* to be a diagnosable herrerasaur outside of Dinosauria (Baron and Williams, 2018), but revising this inference is beyond the scope of our study.

Diagnosis—*Chindesaurus bryansmalli* is diagnosed by a unique combination of character states: smooth proximal surface of the femoral head (lacking a groove), dorsolateral trochanter (= ‘greater trochanter’) of the femur forming a rounded ridge, relatively anteroposteriorly short dorsal centra (centrum length less than 1.33 times the height of the anterior articular surface), and reduced prezygapophyses on the distal caudal vertebrae. The ‘glutealiform’ distal outline of the astragalus used to diagnose *Chindesaurus bryansmalli* by Long and Murry (1995:173) is shared with *Tawa hallae* (see below).

Locality and Horizon—The holotype of *Chindesaurus bryansmalli* (PEFO 10395) was collected from the Upper Triassic

Chinle Formation at PFV 020, Dinosaur Hollow (= PFV 20 of Rob Long’s original numbering scheme; Parker, 2002, 2006) in Petrified Forest National Park, Arizona (Fig. 1; Long and Murry, 1995). In the stratigraphic framework proposed by Martz and Parker (2010) and Martz et al. (2012), PFV 020 lies 34 m below the Black Forest Bed and 1.5 to 3.1 m above Painted Desert Sandstone 3 in the Petrified Forest Member. The age of PFV 020 is bracketed by two maximum deposition ages resulting from U-Pb detrital zircon analyses within the Black Forest bed (209.926 ± 0.072 Ma) and the Petrified Forest Member–Sonsela Member contact (213.124 ± 0.069 Ma; Ramezani et al., 2011). Detailed locality information and field notes are available in the museum archives at PEFO to qualified researchers.

DESCRIPTION

Cervical Vertebrae

One complete cervical centrum (Fig. 2A–C) and half of another are preserved. The length of the complete cervical centrum is less than three times the height of its anterior face. A ventral keel is well developed on its anterior half, but it does not extend onto the most posterior margin of the element (Fig. 2E). Low parapophyses flare out lateral to the anterior edge of the ventral keel, indicating that the only complete cervical centrum from the holotype of *Chindesaurus bryansmalli* came from a more anterior position in the neck than originally proposed (Long and Murry, 1995). Subelliptical shallow excavations (the ‘pleurocoels’ mentioned by Long and Murry, 1995) are located posterodorsal to the low parapophyses (Fig. 2B). The bilateral fossae are subcircular in shape and do not communicate with the hollow interior of the centrum. Such anterior pneumatic fossae are absent in *Herrerasaurus ischigualastensis* (Serenó and Novas, 1994) and *Staurikosaurus pricei* (Bittencourt and Kellner, 2009) but are present in *C. bryansmalli* and *Tawa hallae* (Nesbitt et al., 2009c), *Liliensterius liliensterni* (Huene, 1934), and *Cryolophosaurus ellioti* (Smith et al., 2007). Yet, those taxa lack the second pair of pneumatic fossae on the posterior end of the cervical centra that are found in coelophysoids (Colbert, 1989; Rowe, 1989), *Dilophosaurus wetherilli* (Welles, 1984), and early averostrans such as *Piatnitzky-saurus floresii* (Bonaparte, 1986). The bottom margin of the neural canal is straight and fairly flat. The right side preserves a strong lip on the anterior and ventral margins of the centrum, framed by the top of the parapophysis and the edge of the anterior face of the centrum. Both centrum articular faces are weakly concave. The preserved half of a centrum has a low ventral keel but lacks parapophyses and probably represents the posterior half of the centrum.

Dorsal Vertebrae

Many centra originally assigned to the dorsal series of PEFO 10395 (e.g., Long and Murry, 1995:fig. 177d–h) actually are anterior caudal vertebrae, because the ventral portions of the preserved neural arches lack laminae. We identify five centra that most likely are from the dorsal vertebral series, two of which appear in Figure 2G–R. All are anteroposteriorly short, but dorsoventrally deep, and lack a longitudinal ventral groove and hemal arch articulation facets, which are typically found in caudal vertebrae of other archosaurs. The articular faces of the dorsal centra are wide and slightly concave, not amphiplatyan (contra Long and Murry, 1995). The middle of the centra is mediolaterally narrow laterally, and the ventral margin forms a concave semicircle in lateral view. In dorsal view, the posterior articulation surface for the neural arch forms a broad triangle, but the anterior surface is rectangular. The neural canal is concave ventrally and is deepest in its posterior two-thirds.

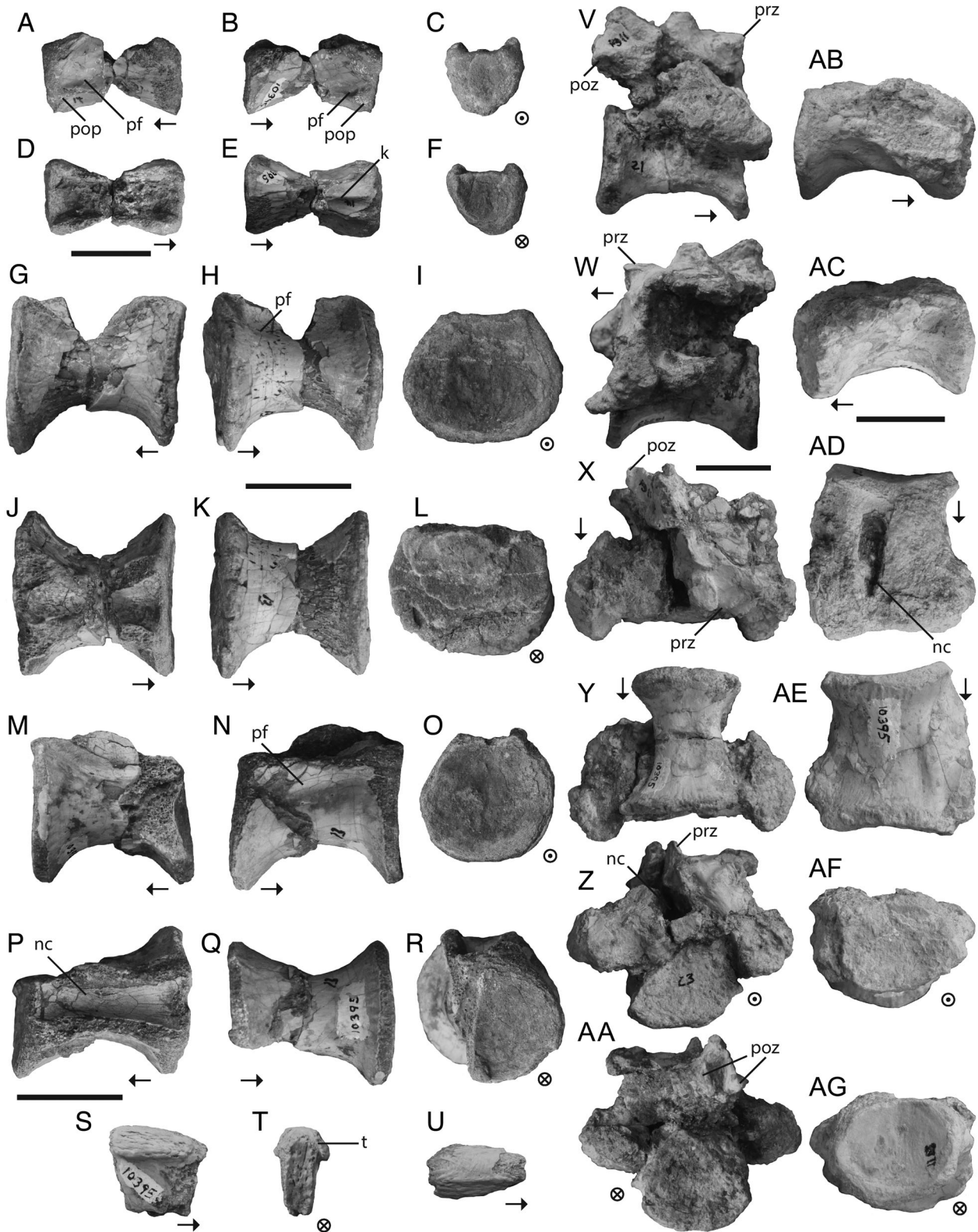


FIGURE 2. *Chindesaurus bryansmalli*, PEFO 10395, holotype, vertebrae. **A–F**, cervical centrum in **A**, left lateral, **B**, right lateral, **C**, anterior, **D**, dorsal, **E**, ventral, and **F**, posterior views. **G–L**, dorsal centrum in **G**, left lateral, **H**, right lateral, **I**, anterior, **J**, dorsal, **K**, ventral, and **L**, posterior views. **M–R**, dorsal centrum in **M**, left lateral, **N**, right lateral, **O**, anterior, **P**, dorsal, **Q**, ventral, and **R**, posterior views. **S–U**, dorsal neural spine in **S**, right lateral, **T**, posterior, and **U**, dorsal views. **V–AA**, sacral vertebra 1 in **V**, right lateral, **W**, left lateral, **X**, dorsal, **Y**, ventral, **Z**, anterior, and **AA**, posterior views. **AB–AG**, sacral vertebra 2 in **AC**, left lateral, **AB**, right lateral, **AF**, anterior, **AD**, dorsal, **AE**, ventral, and **AG**, posterior views. Arrows indicate anterior direction, dot in circle indicates anterior aspect, and cross in circle indicates posterior aspect. **Abbreviations:** **k**, keel; **nc**, neural canal; **pf**, pneumatic fossa; **pop**, parapophysis; **poz**, postzygapophysis; **prz**, prezygapophysis; **t**, table. Scale bars equal 2 cm.

situated on the anterior half of the centrum, whereas the left transverse process is preserved. The anterior edge of the transverse process extends downward to connect with the respective rib via a clear dorsoventral strut of bone. The lateral articular surface of this complex (= transverse process and rib) is 'C'-shaped and opens posteriorly. The anteroventral margin of the rib also expands anteriorly, so that the rib itself has an upside-down 'T'-shaped lateral outline. The sacral ribs are anteroposteriorly flared laterally. The transverse processes are on the same horizontal plane as the prezygapophyses and postzygapophyses. A small depression is found ventrolateral to the prezygapophysis and a small transverse ridge lies underneath the depression (Fig. 2AA), which may represent a hypantrum articulation. The postzygapophyses are found underneath the broad, broken neural spine and extend posteriorly just beyond the posterior face of the centrum.

The centrum of the more posterior sacral vertebra is not co-ossified with its neural arch (Fig. 2AB–AG). The ventral margin of its centrum is less concave than that of the dorsal centra. The anterior face is wider than it is tall and significantly larger than the posterior face. The neural canal is pinched anteriorly and is deepest posteriorly. The neural arch pedicles are thick in dorsal view, and the rib articulation makes up the anterior two-thirds of the sides of the centrum.

Caudal Vertebrae

The largest vertebra of the holotype specimen (Fig. 3A–F) is identified as an anterior caudal vertebra because it lacks neural arch laminae, has a shallow triangular depression on the anterior end of the ventral surface, and its centrum is co-ossified to the neural arch. Two other anterior caudal centra (Fig. 3G–M) are shorter than the preserved dorsal vertebrae, and their ventral margins are less concave than those of the dorsal series when viewed laterally. The neural canal of the best-preserved anterior caudal vertebra is concave and is deepest halfway down the length of the centrum. The articular faces are slightly concave and are only slightly taller than wide. Transverse processes are raised dorsally on the neural arch.

The middle and posterior caudal vertebrae are relatively long and have semicircular concave articular faces (Fig. 3U–AL). The anterior articulation faces slightly ventrally. The ventral edge of the posterior articular face has obvious facets for articulation with the hemal arch (contra Long and Murry, 1995). Three low longitudinal ridges extend along the ventral surface of the more posterior caudal centrum. One traces the midline, and the other two form shallow symmetrical arcs on either side of it. Prezygapophyses and postzygapophyses overhang the centrum in the middle to posterior caudal vertebrae. The transverse processes are flat and are situated in the posterior two-thirds of the vertebral length. These processes project laterally and are oriented posterolaterally like those of many early dinosaurs. A ridge extends from the transverse process to form the ventral margin of the prezygapophysis. A similar ridge extends from the dorsal margin of the prezygapophyses along the length of the vertebra parallel to the neural spine, reaching the dorsolateral edge of the postzygapophyses. The prezygapophyses of the middle and posterior caudal vertebrae are pointed, but the postzygapophyses are rounded. These prezygapophyses do not extend farther anteriorly than 24% of the length of the centrum, unlike *Herrerasaurus ischigualastensis* and *Staurikosaurus pricei*, which have relatively longer prezygapophyses on the posterior caudal vertebrae (Nesbitt, 2011). The neural spine on these vertebrae in *Chindesaurus bryansmalli* is long and begins rising just posterior to where the prezygapophyses meet the neural arch. The spine remains low until two-thirds of its anteroposterior length, after which it rises up to form a small table with a pair of posterior rounded projections at its tip (Fig.

3AE). A triangular spinopostzygapophyseal fossa (Fig. 3Z, AF, AL; Wilson et al., 2011), or the 'postspinal chonos' of Welles (1984:94), is located between the postzygapophyses at the base of the neural spine (bounded by the intrapostzygapophyseal lamina and spinopostzygapophyseal laminae; Wilson, 1999). The neural canal is almost entirely restricted to the neural arch and barely excises the top of the centrum.

Hemal Arches

The preserved chevrons are concave posteriorly in dorsal view, and the proximal end is faceted to articulate with the caudal centra (Fig. 3O–T). The arch on either side of the hemal canal is ridged anteriorly, but smooth posteriorly. Larger chevrons are anteroposteriorly expanded just below the proximal end and also distally.

Ilium

The posterior left iliac blade fragment preserves a dorsolateral triangular rugosity that makes up much of the anterior half of the lateral surface of that fragment (Fig. 4B–G). The original description (Long and Murry, 1995) mentioned that this rugosity was shared between *Chindesaurus bryansmalli* and *Caseosaurus Crosbyensis* (UMMP 8870; Hunt et al., 1998). Subsequent authors confirmed that this feature was indeed shared between the two taxa (Fig. 5A; Nesbitt et al., 2007; Baron and Williams, 2018), but we agree with those authors in not synonymizing these taxa owing to their highly incomplete nature. A horizontal ridge projects medially from the postacetabular process (Fig. 4C, E). This structure represents the platform that is positioned ventral to the articulation of the transverse process of the last fully sacral vertebra. A well-developed brevis fossa is not present on the ilium of *C. bryansmalli*, although this region is not well preserved. Another piece of the dorsal blade of the ilium is also preserved but it is uninformative (Fig. 4H–J).

The right ischiadic peduncle of the ilium is flat medially and is anteroposteriorly expanded at its distal end (Fig. 4K–N). A shallow anterior concavity represents the acetabular margin of the ischiadic peduncle (Fig. 4K–L). The overall size and shape of this element is difficult to interpret. Both pubic peduncles are preserved (Fig. 4O–Z) and have flat medial sides. The distal end is expanded anteroposteriorly and is 'kinked,' forming two flat surfaces. The larger surface faces ventrally, and the smaller surface faces anteroventrally. The angle formed by these surfaces on the anteroventral margin of the pubic peduncle is ca. 120° in lateral view. In distal view, the pubic peduncle is subtriangular; the lateral apex of the triangle is the ridge that forms the outer rim of the acetabulum. The fossa that represents the medial acetabular wall on the pubic peduncle and its concave posterior margin suggests that the acetabulum was at least partially open. The supraacetabular crest terminates before the distal end of the pubic peduncle in *C. bryansmalli* (Fig. 4O, U) and neotheropods but extends to the distal extremity of the pubic peduncle in herrerasaurids (Nesbitt and Ezcurra, 2015).

Pubis and Ischium

The proximal surface of the pubis is flat medially and has a convex anterolateral surface that becomes flat posterolaterally (Fig. 6A–D). The iliac pedicle of the pubis is lateromedially wide where it would have articulated with the ilium. The ischiadic pedicle is broken off, but part of the articulation surface for the femur is visible at a different angle posterior to the iliac articulation. A smooth semicircular concavity is found distal to the broken ischiadic pedicle on the lateral surface of the bone, representing the anterior half of the obturator foramen. The pubic shaft is nearly straight (it arches slightly inward) and

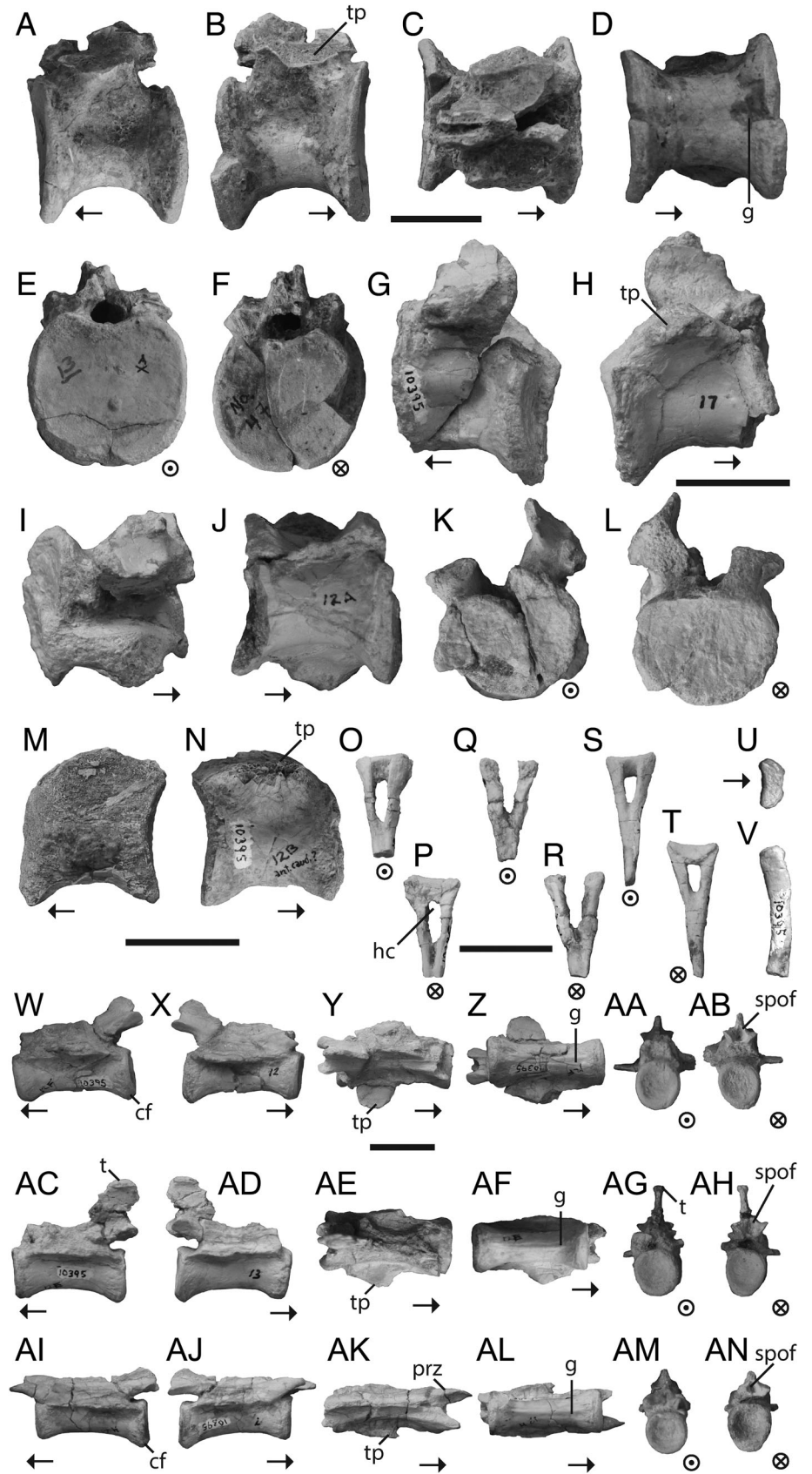


FIGURE 3. *Chindesaurus bryansmalli*, PEFO 10395, holotype, caudal vertebrae. **A–F**, anterior caudal vertebra in **A**, left lateral, **B**, right lateral, **C**, dorsal, **D**, ventral, **E**, anterior, and **F**, posterior views. **G–L**, anterior caudal vertebra in **G**, left lateral, **H**, right lateral, **I**, dorsal, **J**, ventral, **K**, anterior, and **L**, posterior views. **O–P**, hemal arch in **O**, anterior and **P**, posterior views. **Q–R**, hemal arch in **Q**, anterior and **R**, posterior views. **S–V**, hemal arch in **S**, anterior, **T**, posterior, **U**, dorsal, and **V**, right lateral views. **W–AB**, posterior caudal vertebra in **W**, left lateral, **X**, right lateral, **Y**, dorsal, **Z**, ventral, **AA**, anterior, and **AB**, posterior views. **AC–AH**, posterior caudal vertebra in **AC**, left lateral, **AD**, right lateral, **AE**, dorsal, **AF**, ventral, **AG**, anterior, and **AH**, posterior views. **AI–AN**, posterior caudal vertebra in **AI**, left lateral, **AJ**, right lateral, **AK**, dorsal, **AL**, ventral, **AM**, anterior, and **AN**, posterior views. Arrows indicate anterior direction, dot in circle indicates posterior aspect, and cross in circle indicates posterior aspect. **Abbreviations:** **cf**, chevron facet; **g**, groove; **hc**, hemal canal; **prz**, prezygapophysis; **spof**, spinopostzygapophyseal fossa; **t**, table; **tp**, transverse process. Scale bars equal 2 cm.

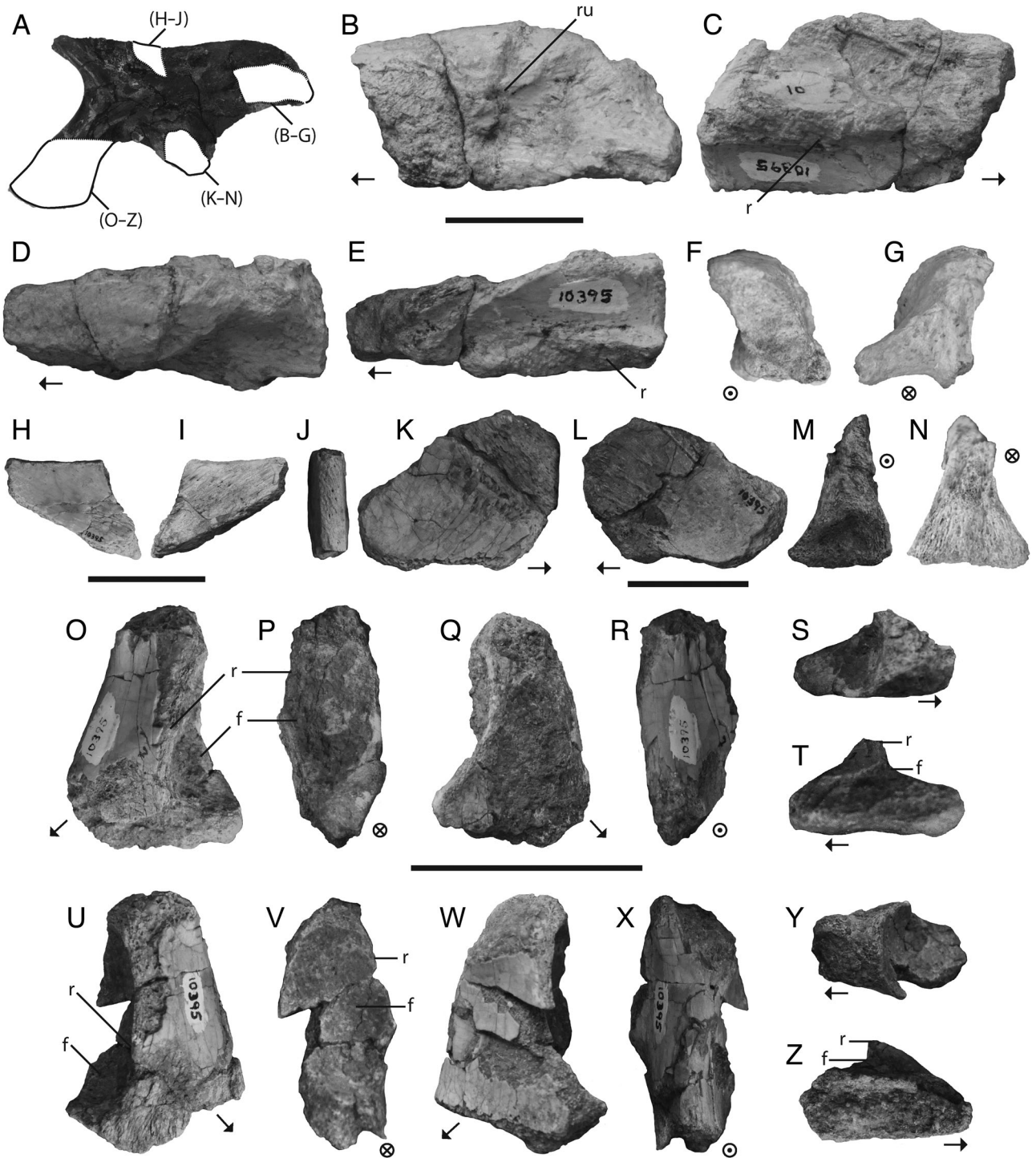


FIGURE 4. *Chindesaurus bryansmalli* pelvis with *Tawa hallae* ilium for comparison. **A**, *Tawa hallae* ilium GR 1062 **B–Z**, *Chindesaurus bryansmalli*, PEFO 10395, pelvic elements. **B–G**, fragmentary left postacetabular process in **B**, lateral, **C**, medial, **D**, dorsal, **E**, ventral, **F**, anterior, and **G**, posterior views. **H–J**, dorsal margin of the iliac blade in **H**, lateral, **I**, medial, and **J**, dorsal views. **K–N**, right ischiadic peduncle in **K**, lateral, **L**, medial, **M**, anterior, and **N**, posterior views. **O–T**, left pubic peduncle in **O**, lateral, **P**, posterior, **Q**, medial, **R**, anterior, **S**, proximal, and **T**, distal views. **U–Z**, right pubic peduncle in **U**, lateral, **V**, posterior, **W**, medial, **X**, anterior, **Y**, proximal, and **Z**, distal views. Arrows indicate anterior direction, dot in circle indicates anterior aspect, and cross in circle indicates posterior aspect. **Abbreviations:** f, fossa; r, ridge; ru, rugosity. Scale bars equal 2 cm.

lacks the distal end. In proximal view, the broken shaft is subcircular but transitions to subelliptical in more distal cross-section (Fig. 6E, F). The base of the anteroposteriorly narrow pubic apron (Novas, 1997) is present along the length of the bone,

but its medial margin is broken. The proximal end of the pubic apron is pointed posteromedially in proximal view. The fragment interpreted here as the distal end of the ischium (Fig. 6G–L) is worn but has a flattened medial surface that

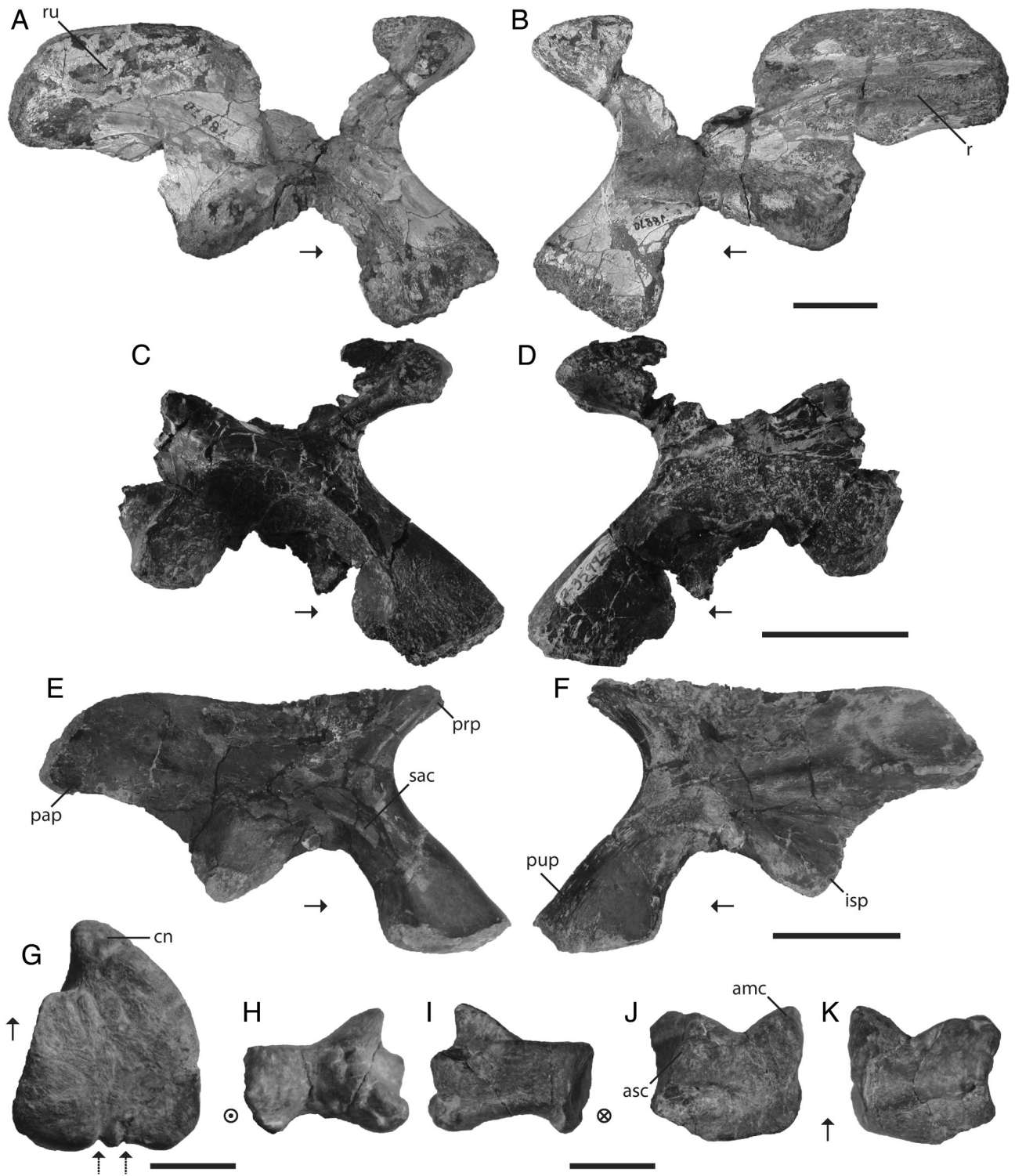


FIGURE 5. **A–B**, *Caseosaurus crosbyensis*, UMMP 8870, holotype, right ilium in **A**, lateral and **B**, medial views. **C–D**, *Caseosaurus*, NMMNH P-35996, right ilium in **C**, lateral and **D**, medial views. **E–J**, select elements from *Tawa hallae*, GR 1062, left ilium (reversed) in **E**, lateral and **F**, medial views. **G**, GR 242, left tibia, in proximal view. **H–K**, GR 242, left astragalus in **H**, anterior, **I**, posterior, **J**, proximal, and **K**, distal views. Solid arrows indicate anterior direction, dot in circle indicates anterior aspect, and cross in circle indicates posterior aspect. Dashed arrows indicate the two notches in the posterior edge of the proximal surface of the tibia. **Abbreviations:** **amc**, anteromedial corner; **asc**, ascending process; **cn**, cnemial crest; **isp**, ischiac peduncle; **lc**, lateral condyle; **mc**, medial condyle; **pop**, postacetabular process; **prp**, preacetabular process; **pup**, pubic peduncle; **r**, ridge; **ru**, rugosity; **sac**, supraacetabular crest. Scale bars equal 1 cm (**A–F**) and 2 cm (**G–K**).

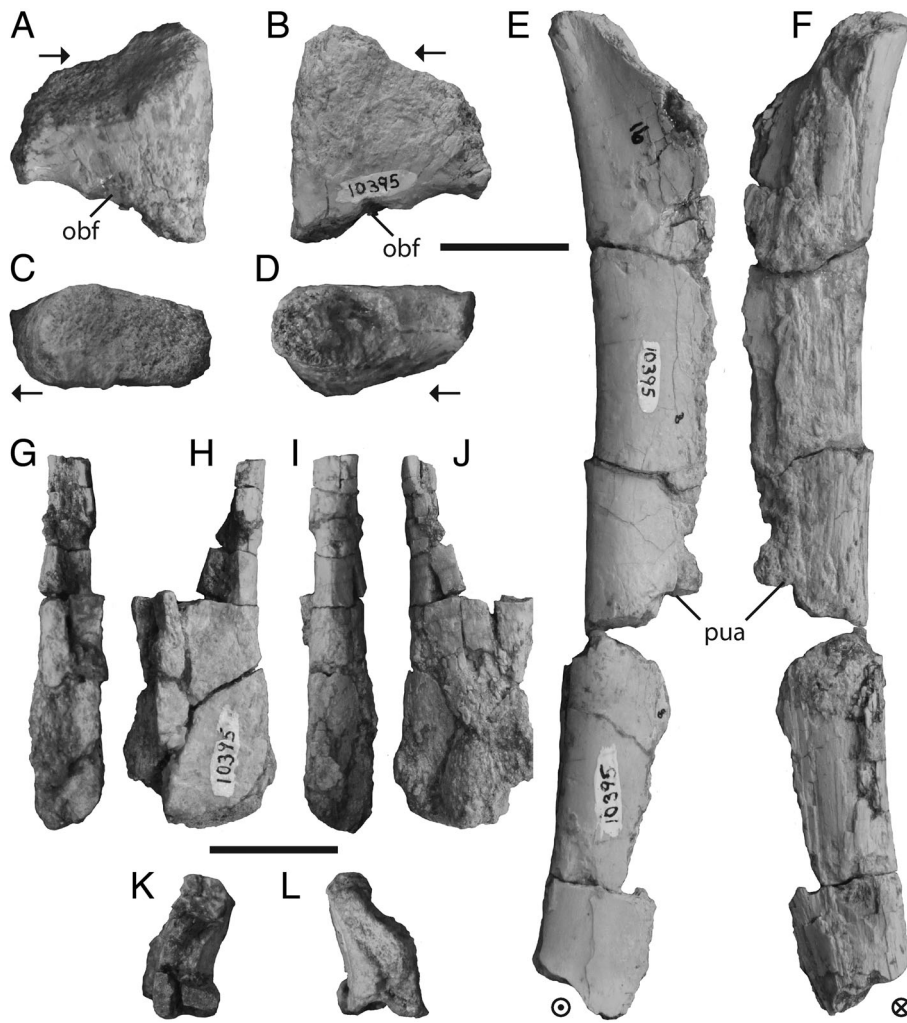


FIGURE 6. *Chindesaurus bryansmalli*, PEFO 10395, holotype, pelvic elements. **A–F**, right pubis in **A**, lateral, **B**, medial, **C**, proximal, **D**, distal, **E**, anterior, and **F**, posterior views. **G–J**, distal end of ischium in four views (uncertain) and in **K**, proximal and **L**, distal views. Arrows indicate anterior direction, dot in circle indicates anterior aspect, and cross in circle indicates posterior aspect. **Abbreviations:** **obf**, margin of obturator foramen; **pua**, pubic apron. Scale bars equal 2 cm.

articulated with its counterpart. The proximal margin of the element is flat and thinner than the distal end, which is expanded anteroposteriorly.

Femur

The right femur of PEFO 10395 is nearly complete (Fig. 7A–G), whereas only the proximal portion of the left femur (Fig. 7H–K) is preserved. The bone is subelliptical in proximal view, with a rounded medial margin and a tapering and posteriorly curving lateral portion that corresponds to the dorsal surface of the greater trochanter. The posterior surface of the femoral head is mostly smooth and flat, but its proximal part contains a small rugose surface (Fig. 7A–E, H–L). The femoral head turns laterally abruptly and forms a rounded proximolateral corner in anterior view. The head has a subrectangular medial outline and is flat dorsally, anteriorly, and posteriorly. Best seen in proximal (Fig. 7E, L) and posterior (Fig. 7C, J) views, the femora of *Chindesaurus bryansmalli* lack a strong anteromedial tuber (Fig. 7E, L), which forms a lip on the posteromedial surface of the bone in neotheropods (Nesbitt et al., 2011), but it has a well-developed facies articularis antitrochanterica lateral to that. The ventral surface of the femoral head is excavated by the distal extension of the ligament sulcus lateral to a small ventrally directed hooked lip. The dorsolateral trochanter (= greater

trochanter) forms a rounded ridge (Fig. 7B) that extends parallel to the lateral margin of the head on the lateral portion of the anterior surface. A sinusoidal groove separates the dorsolateral trochanter from the anterior trochanter and trochanteric shelf. The structure formed by the anterior trochanter and trochanteric shelf is triangular in anterior view, and the anterior trochanter lies on the medial half of the anterior surface of the proximal part of the shaft (Fig. 7A, H). The anterior trochanter points proximally but is not separated from the shaft by a cleft, as it is in some specimens of coelophysoids such as ‘*Syntarsus*’ *kayentakatae* (Rowe, 1989) and *Dilophosaurus wetherilli* (Welles, 1984). A lateral concavity marks the posteroproximal edges of the proximodistally oriented anterior trochanter and the trochanteric shelf, which extends posterolaterally perpendicular to anterior trochanter. The proximal surface of the trochanteric shelf forms a 98° angle with the long axis of the femoral shaft. Some specimens previously referred to *C. bryansmalli* lack a trochanteric shelf (Fig. 8A, F, K). The femoral shaft is sigmoidal in anterior and posterior views; the proximal half bows out laterally and the distal half arches medially, where the inflection point is just below the distal terminus of the fourth trochanter. In lateral and medial views, the femoral shaft is slightly arched anteriorly. Although incomplete, the fourth trochanter can be reconstructed as slightly convex medially and asymmetrical in profile. An oval pit is found anterior to the fourth trochanter.

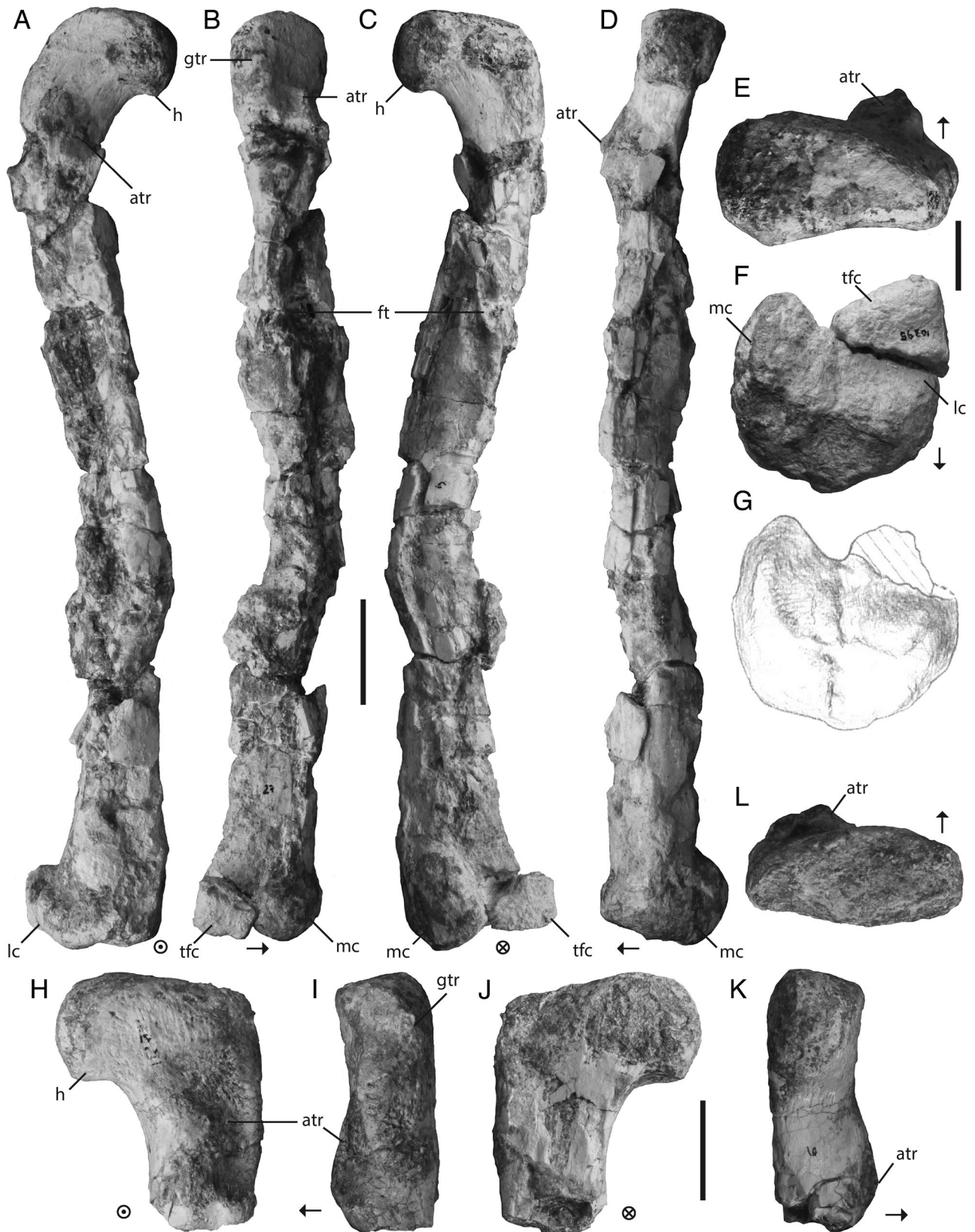


FIGURE 7. *Chindesaurus bryansmalli*, PEFO 10395, holotype, femora. **A–G**, right femur in **A**, anterior, **B**, lateral, **C**, posterior, **D**, medial, **E**, proximal, and **F, G**, distal views. **H–L**, fragmentary left femur in **H**, anterior, **I**, lateral, **J**, posterior, **K**, medial, and **L**, proximal views. **G** is modified from Long and Murry, 1995, and shows the element prior to additional preparation. Arrows indicate anterior direction, dot in circle indicates posterior aspect, and cross in circle indicates posterior aspect. **Abbreviations:** atr, anterior trochanter; ft, fourth trochanter; gtr, 'greater' (= dorsolateral) trochanter; h, head; lc, lateral condyle; mc, medial condyle; tfc, tibiofibular crest. Scale bars equal 2 cm.

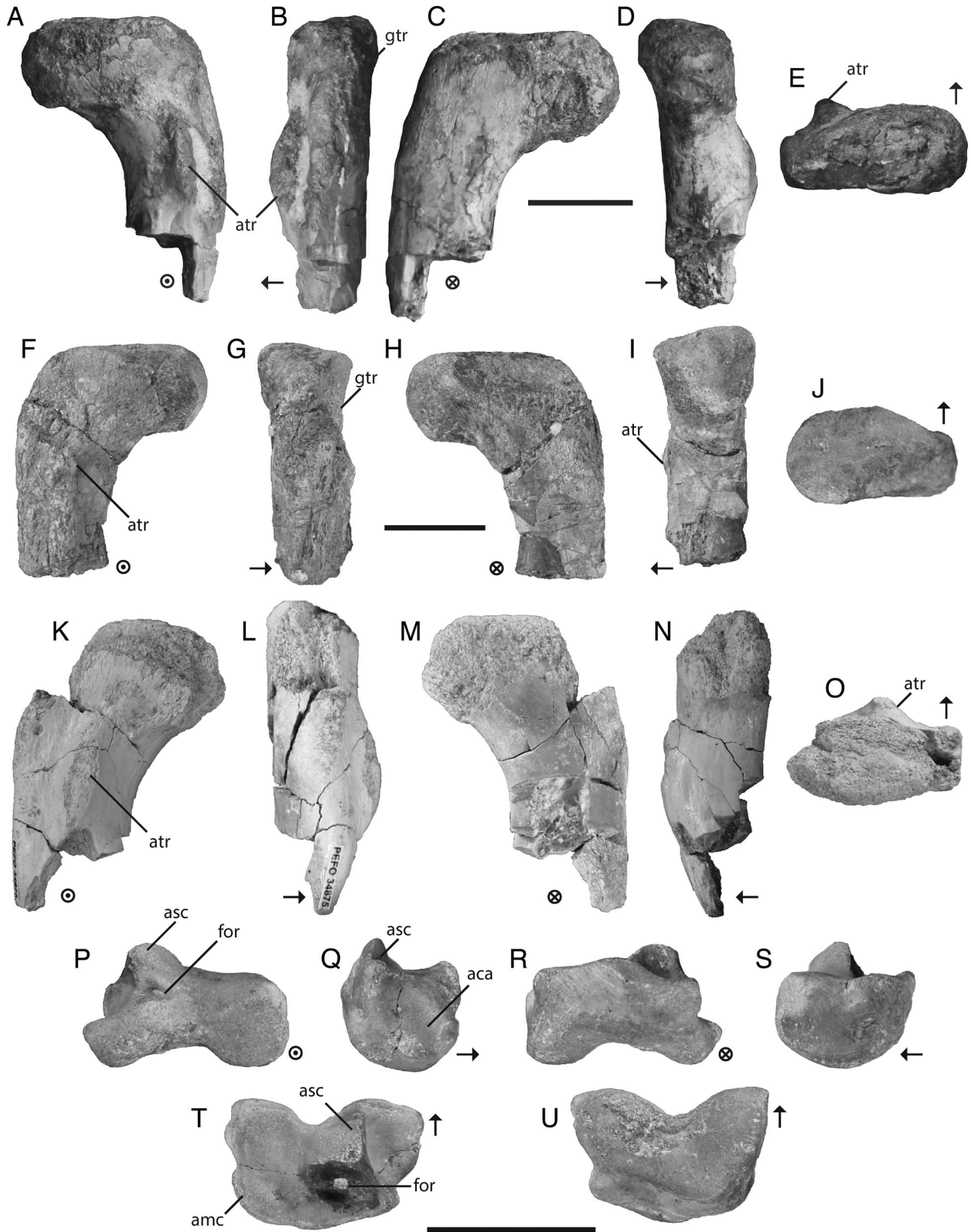


FIGURE 8. *Chindesaurus bryansmalli* from Petrified Forest National Park, select referred specimens. **A–F**, PEFO 33982, proximal end of a right femur, in **A**, anterior, **B**, lateral, **C**, posterior, **D**, medial, and **E**, proximal views. **F–J**, PEFO 40754, proximal end of left femur, in **F**, anterior, **G**, lateral, **H**, posterior, **I**, medial, and **J**, proximal views. **K–O**, PEFO 34875, proximal end of left femur, in **K**, anterior, **L**, lateral, **M**, posterior, **N**, medial, and **O**, proximal views. **P–U**, PEFO 40753, right astragalus from the *Chindesaurus* + *Tawa* clade, in **P**, anterior, **Q**, lateral, **R**, posterior, **S**, medial, **T**, proximal, and **U**, distal views. Arrows indicate anterior direction, dot in circle indicates anterior aspect, and cross in circle indicates posterior aspect. **Abbreviations**: **aca**, articular surface for the calcaneum; **amc**, anteromedial corner; **asc**, ascending process; **atr**, anterior trochanter; **for**, foramen; **gtr**, ‘greater’ (= dorsolateral) trochanter. Scale bars equal 2 cm.

The distal end of the right femur (Fig. 7F, G) has been repaired since it was last figured and described by Long and Murry (1995). The broken posterolateral corner has been readhered to the fossil, restoring the lateral condyle and tibiofibular crest. As in *Herrerasaurus ischigualastensis* (Novas, 1993), *Staurikosaurus pricei* (Galton, 1977), and *Tawa hallae* (Nesbitt et al., 2009c), the lateral condyle and tibiofibular crest are not well differentiated from one another in distal view and combined make up a larger structure that projects more posteriorly than the medial condyle. The lateral and medial distal articular surfaces are separated by a shallow groove that continues up the posterior surface. The distal outline of the medial condyle is subelliptical, and in posterior view the condyle is fairly tall and tapers proximally. The lateral condyle and tibiofibular crest are subrhomboidal and flat distally. Those structures form a low triangle in posterior view, and a short, angled ridge touches the apex of this triangle and extends proximally.

Tibia

The right tibia of PEFO 10395 is badly crushed and preserves portions of the proximal and distal ends (Fig. 9). The proximal end expands mediolaterally and is flat. The cnemial crest is incomplete, but it extends down the shaft and points anterolaterally. The anterolateral margin of the proximal surface is also incomplete, so the proximal outline of the bone is uncertain. A ‘U’-shaped notch separates the lateral and medial proximal condyles posteriorly and, like in *Tawa hallae*, a second smaller notch is present lateral to that (Figs. 5G, 9A, B). Proximally, the lateral condyle is much larger in area than the medial condyle. The posterior margin of the lateral condyle is straight. Short longitudinal striations begin on the posterior end of the proximal surface and extend down the posterior surface of the proximal end of the tibia. The distal end of the tibia has a proximodistally oriented groove on its lateral surface, and the anterolateral process is broken and incomplete. The distal articular surface for the astragalus is flat at the posterolateral process but is convex medially. In anterior view, the broken base of the broken anterolateral process forms a straight shelf extending proximolaterally from the mediolateral corner of the bone (Fig. 9G). That shelf represents the edge of the articular surface of the missing anterolateral process. The posterolateral process tapers significantly distolaterally (Fig. 9F); it projects distally and laterally farther than the rest of the distal end of the tibia and forms a pointed maleolus similar to that of *T. hallae*, *Guaibasaurus candelariensis*, and *Lesothosaurus diagnosticus* (Langer et al., 2011, 2016; Baron et al., 2017c). The anterior surface of the posterolateral process is concave in distal view. In that view, the anteromedial corner of the bone forms a 90° angle, whereas the posteromedial corner is rounded. Part of the posteromedial corner is broken.

Astragalus

The astragalus (Fig. 9J–O) is broken along the posterolateral margin, and the lateral end is broken such that the contact with the calcaneum is incomplete (Nesbitt et al., 2007). The medial surface is semicircular and flat. In distal view, the posterior margin is straight, but the anterior margin is concave, forming an obtuse angle between a large medial condyle and the triangular incomplete lateral condyle, similar to the astragalus of *Tawa hallae* (Fig. 5J). In anterior view, the groove between these two condyles actually continues on the distal surface of the bone in the holotype of *Chindesaurus bryansmalli* (Fig. 9J), dividing it into unequal regions. That ‘V’-shaped groove (Fig. 9N) is what gives this element the ‘glutealiform’ appearance noted by Long and Murry (1995). *Herrerasaurus ischigualastensis* and neotheropods exhibit a much shallower version of that groove, and sauropodomorphs have flat roller-shaped distal astragalus surfaces. A

subtriangular fossa (= astragalus cranial platform of Langer, 2003) is present lateral to the proximal extent of the distal groove in anterior view. A circular foramen perforates that fossa beneath the anterolateral ascending process of the astragalus. That process is triangular in lateral/medial views and capped by an anteroproximally facing flat surface that would articulate with the anterolateral process of the tibia. A basin for the articulation of the posterolateral process of the tibia is posterior to the ascending process, and another circular foramen lies at the bottom of that depression. A ridge extends posteromedially from the posterior margin of the ascending process, setting the above-mentioned basin apart from another depression, which occupies the posterior part of the medial surface of the astragalus. That ridge ends in a low triangle at the posterior margin of the astragalus. A subelliptical fibular notch is visible lateral to the ascending process and dorsal to the broken lateral surface.

PHYLOGENETIC ANALYSES

Parsimony Analysis

We included only the holotype specimen of *Chindesaurus bryansmalli* (PEFO 10395) into a character-taxon matrix constructed by Nesbitt et al. (2009c) and modified by Ezcurra and Brusatte (2011) and Nesbitt and Ezcurra (2015). We modified the states of three characters (336, 342, and 343), rescored taxa for those characters, and added nine characters (characters 344–352; see Supplemental Data 1 for complete character descriptions and taxon scores). This particular data set was chosen for the analysis because it includes a broad sampling of operational taxonomic units (OTUs) within groups to which *C. bryansmalli* previously was hypothesized to belong (e.g., non-dinosaurian Dinosauromorpha, Herrerasauridae, Sauropodomorpha, non-neotheropod Theropoda) and includes some of the most up-to-date character scores for the taxa in the matrix. Only the holotype specimen of the neotheropod *Lepidus praecisio*, TMM 41936-1.3 (Nesbitt and Ezcurra, 2015), was included in our analysis. The final matrix comprises 352 characters and 45 species-level taxa (the TNT file and most parsimonious trees [MPTs] are available in MorphoBank (<http://morphobank.org/permalink/?P3384>)). Characters 17, 30, 67, 128, 174, 184, 213, 219, 231, 236, 248, 253, 254, 273, 329, and 343 were ordered, and all characters were weighted equally. *Erythrosuchus africanus* and *Euparkeria capensis* serve as the immediate outgroups to Archosauria in this analysis (Nesbitt et al., 2009c). The matrix was constructed in Mesquite (Maddison and Maddison, 2015), and an equal-weight parsimony analysis was performed in TNT (Goloboff et al., 2008). The phylogenetic analysis utilized a heuristic search of Wagner trees with 1,000 repetitions and randomly added sequences before tree bisection and reconnection branch swapping. Ten trees were held for each replicate, and zero-length branches were collapsed.

The resulting two MPTs had lengths of 1,086 steps, a consistency index of 0.390, and a retention index of 0.685. The best tree score was hit in every replication. In the strict consensus tree, we find *Chindesaurus bryansmalli* removed from a monophyletic Herrerasauridae (*Herrerasaurus ischigualastensis* + *Staurikosaurus pricei*) and pulled crownward up the tree as the sister taxon of *Tawa hallae* (Fig. 10). The *Chindesaurus bryansmalli* + *Tawa hallae* clade and Herrerasauridae are both included within Theropoda but along with *Eodromaeus murphi* are excluded from Neotheropoda. Theropoda is supported by 11 apomorphies (common to both MPTs), and the node representing the most recent common ancestor of *Chindesaurus bryansmalli* and all other theropods is united by seven apomorphies (apomorphy lists are provided in Supplemental Data 1). The *Chindesaurus bryansmalli* + *Tawa hallae* sister relationship is also supported by seven apomorphies. Neotheropoda (Coelophysoidea + stem

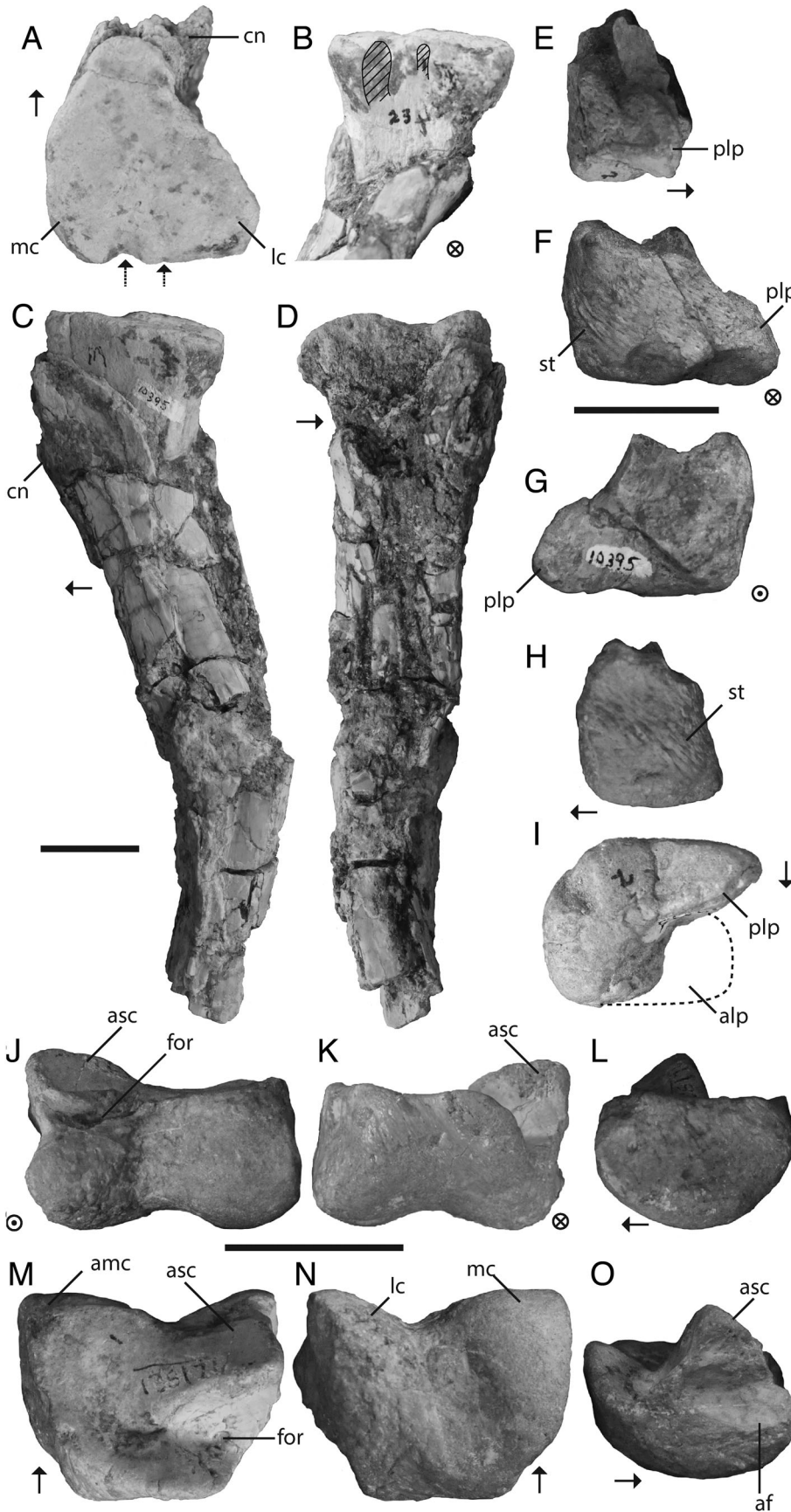


FIGURE 9. *Chindesaurus bryansmalli*, PEFO 10395, holotype, hind limb elements. **A–I**, right tibia and **J–O**, right astragalus in **A**, **M**, proximal, **B**, **F**, **K**, posterior, **C**, **H**, **L**, medial, **D**, **E**, **O**, lateral, **G**, **J**, anterior, and **I**, **N**, distal views. Solid arrows indicate anterior direction, dot in circle indicates anterior aspect, and cross in circle indicates posterior aspect. Dashed arrows and areas indicate the two notches in the posterior edge of the proximal surface of the tibia. **Abbreviations:** af, articular surface for fibula; alp, anterolateral process; amc, antero-medial corner; asc, ascending process; cn, cnemial crest; for, foramen; lc, lateral condyle; mc, medial condyle; plp, posterolateral process; st, striations. Scale bars equal 2 cm.

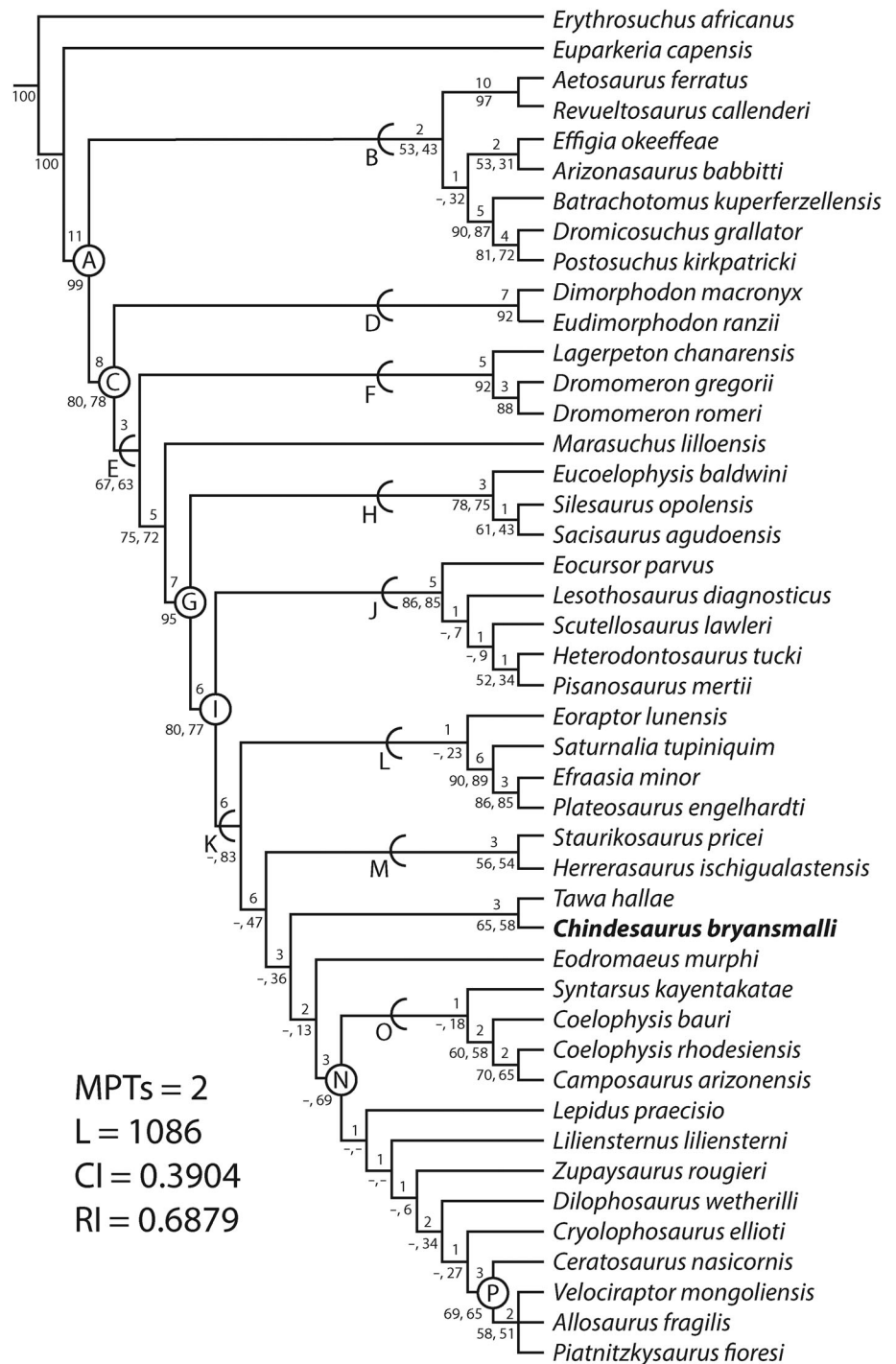


FIGURE 10. Strict consensus tree resulting from the two MPTs recovered in the phylogenetic analysis. Numbers above each node reflect Bremer support values, and numbers below the node represent bootstrap scores as (absolute bootstrap, GC bootstrap). Clades that were not reconstructed in the bootstrap analyses are marked with an ‘-’, and only one bootstrap score is reported where the two analyses calculated the same score. **Abbreviations:** A, Archosauria; B, Pseudosuchia; C, Ornithodira; D, Pterosauria; E, Dinosauromorpha; F, Lagerpetidae; G, Dinosauriformes; H, Silesauridae; I, Dinosauria; J, Ornithischia; K, Saurischia; L, Sauropodomorpha; M, Herrerasauridae; N, Neotheropoda; O, Coelophysoidea; P, Averostra.

averostrans + Averostra in this analysis) is supported by 16 apomorphies.

Sensitivity Analyses

In order to better understand the effect of fragmentary specimens and missing data on our phylogenetic results, we first calculated the percent completeness for each character (how many taxa were scored for a given character) and for each taxon (how many characters were scored for a given taxon) in the

matrix (Supplemental Data 2). Then, we iteratively removed the most incomplete taxon and reran the tree search using the same parameters given above, calculating GC bootstrap values for the nodes in the recovered consensus trees. In effect, we reran the original analysis (1) first without *Dromomeron gregorii*, then (2) without *D. gregorii* and *Camposaurus arizonensis*, and finally (3) without *D. gregorii*, *Ca. arizonensis*, and *Eucoelophysis baldwini*. The results of these sensitivity analyses are shown in Figure 11 and Supplemental Data 2; support for Coelophysoidea was not considered in these analyses because it was not recovered

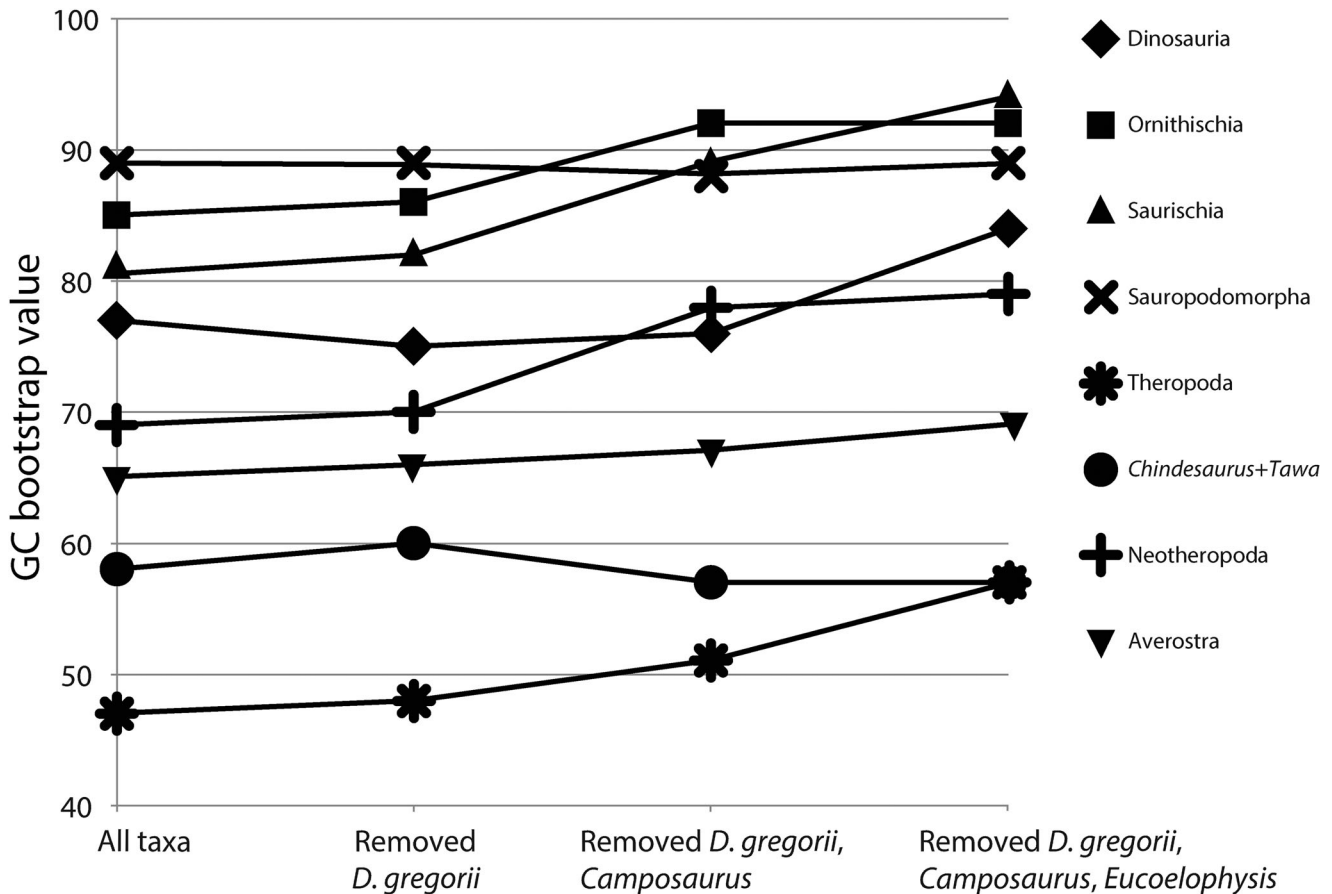


FIGURE 11. Increased node support by iteratively removing incomplete taxa in the sensitivity analyses. The horizontal-axis labels refer to the analyses discussed in the text that iteratively removed the incomplete taxa *Dromomeron gregorii*, *Camposaurus arizonensis*, and *Eucoelophysys baldwini*.

with the same membership during the resampling. All four analyses resulted in two MPTs, with the non-omitted taxa keeping congruent positions across the analyses, that consequently decreased in length from 1,086 to 1,080 steps (Supplemental Data 1). The GC bootstrap values for Dinosauria dropped 1% from 80% between A and A' but rose to 84% when all three taxa were excluded (Fig. 11). The support for the *Chindesaurus bryansmalli* + *Tawa hallae* clade ranged between 57% and 60% and was highest when only *D. gregorii* was removed. The support for Sauropodomorpha did not change much between 88% and 89%. All of the other clades considered in the sensitivity analyses increased in support as each taxon was removed. The largest increases in GC bootstrap values occurred in Saurischia (from 83% to 94%). Support for Theropoda and Neotheropoda each increased by 10% during the analyses (from 47% to 57% and from 69% to 79%, respectively), and that for Ornithischia increased by 7% (from 85% to 92%). The group that changed the least (smallest increase in GC bootstrap) was Averostra (from 65% to 69%).

DISCUSSION

Revised Diagnosis

The sister-taxon relationship of *Chindesaurus bryansmalli* and *Tawa hallae* recovered in this study was also recently found in other analyses (e.g., Langer and Bittencourt, 2014; Cabreira et al., 2016; Baron et al., 2017b). We refrain from naming this

group owing to the fact that it only includes taxa that could be separated in future analyses by the discovery of more complete specimens or novel characters or taxa. That said, both *C. bryansmalli* and *T. hallae* are diagnosable based on several anatomical differences and remain as valid taxa. The holotype specimen of *C. bryansmalli* is diagnosed by a unique combination of four character states: smooth proximal surface of the femoral head, lacking a groove (shared with aetosaurs, pterosaurs, lagerpetids, *Lesothosaurus diagnosticus*, and averostran theropods); 'dorsolateral trochanter' of the femur forming a rounded ridge (shared with sauropodomorphs and coelophysoids); relatively short dorsal centra (centrum length less than 1.33 times the height of the anterior articular surface; shared with other theropods but not *T. hallae* or coelophysoids); and short prezygapophyses on the distal caudal vertebrae (plesiomorphic for dinosaurs but not found in pterosaurs or other theropods). With respect to the above characters, *Tawa hallae* has a curved transverse groove on the proximal surface of the femur, a 'dorsolateral trochanter' on the proximal end of the femur formed by a sharp ridge, and relatively longer dorsal centra and prezygapophyses on the distal caudal vertebrae compared with those of *C. bryansmalli*. *Tawa hallae* is similarly diagnosed by a unique combination of three character states: middle portion of ventral keel of cervical centra is ventral to the centrum rims (shared with *Effigia okeeffeae*, *Eocursor parvus*, and *Herrerasaurus ischigualastensis*), femoral head orientation is medial and the angle with respect to the transverse axis through the femoral condyles is less than 20° (shared with tetanurans), and the absence of an

anterior trochanteric shelf (the plesiomorphic condition that may be ontogenetically variable; Griffin and Nesbitt, 2016a, 2016b; Evans et al., 2018).

The *Chindesaurus bryansmalli* + *Tawa hallae* clade is diagnosed by one apomorphy, the posterior margin of the proximal end of the tibia is divided by two notches (see Figs. 5G, 9A, B), and a unique combination of five character states: the oblique ligament sulcus on the posterior surface of the femoral head is absent (this sulcus is present in *Herrerasaurus ischigualastensis* and other dinosaurs; Novas, 1993; Rauhut, 2003; Nesbitt and Chatterjee, 2008), the cnemial crest makes up <35% of the total anteroposterior width of the tibia in proximal view (shared with *Dromomeron romeri* and *Efraasia minor*), the posterolateral process of the tibia tapers while projecting laterodistally (shared with *Lesothosaurus diagnosticus*; see Description), the proximal outline of the astragalus is relatively short such that the anteroposterior-mediolateral width is >0.7 (shared with some ornithischians such as *Scutellosaurus lawleri*), and the anterior margin of the astragalus is strongly concave and is continuous with an anteroposterior concavity on the distal surface (= ‘glutealiform’ shape of Long and Murry, 1995; shared with *Dimorphodon macronyx* and *Marasuchus lilloensis*; see Figs. 5H–K, 8P–U, 9J–O). Right tibiae (TTU-P11044 and TTU-P11175) from the Cooper Canyon Formation of Garza County, Texas (Nesbitt and Chatterjee, 2008; Sarigiül, 2017), may be referred to this clade owing to the presence of two notches on the posterior margin of the proximal end of the tibia.

The *Chindesaurus bryansmalli* + *Tawa hallae* Clade

Except for the holotype specimen of *Chindesaurus bryansmalli* (PEFO 10395), other published specimens referred to the taxon are isolated and often incomplete elements, a taphonomic bias that excludes the possibility of preserving the unique combination of character states that diagnose the taxon. The fact that the holotype specimens of *C. bryansmalli* and *Tawa hallae* are morphologically similar enough to one another to form a clade in a parsimony analysis suggests that these two taxa belong to the same evolutionary lineage, and it may be difficult or impossible to identify isolated specimens to one taxon or the other. This is especially true given that many of the features that diagnose *C. bryansmalli* and *T. hallae* (and their respective clades) have recently been shown to be ontogenetically variable in early dinosaurs and their immediate outgroups (Griffin and Nesbitt, 2016a, 2016b; Evans et al., 2018; Nesbitt et al., 2018). This problem is not unique to early dinosaurs; other important Triassic taxa such as the archosauriform *Vancleavea campi* (Long and Murry, 1995) and the crocodylomorph *Hesperosuchus agilis* (Colbert, 1952) also have incomplete holotype specimens that are difficult to diagnose (Walker, 1970; Parker and Barton, 2008), more complete skeletons of anatomically similar individuals (Parrish, 1991; Clark et al., 2000; Nesbitt et al., 2009a), and long stratigraphic ranges (Parker, 2006; Parker and Martz, 2011; Morris and Werning, 2012) that make it difficult to assess the alpha taxonomy within their respective groups.

Although its current members are North American (including the possible referred specimens TTU-P11044 and TTU-P11175), the *Chindesaurus bryansmalli* + *Tawa hallae* clade may also include *Guibasaurus candelariensis*, a problematic early dinosaur from the Caturrita Formation of southern Brazil (Bonaparte et al., 1999, 2007; Langer et al., 2011). *Guibasaurus candelariensis* was not included in this study, but it shares a tapering posterolateral process of the distal end of the tibia with *C. bryansmalli* and *T. hallae* (Langer et al., 2016). *Chindesaurus bryansmalli* has been suggested to possess a much broader geographic and stratigraphic range than *T. hallae*, because the latter is so far only known from its type locality in the Hayden Quarry at Ghost Ranch, New Mexico (Fig. 1). In contrast, specimens referred to

C. bryansmalli have been found in the Petrified Forest Member (PFV 020; Long and Murry, 1995) and Sonsela Member (PFV 89) of the Chinle Formation at Petrified Forest National Park, the Petrified Forest Member at Ghost Ranch, New Mexico (occurring in the same quarry as *T. hallae*, Hayden Quarry Site 2; Irmis et al., 2007; Nesbitt et al., 2009c), and the Colorado City Formation (Otis Chalk Quarry 3, TMM 31100/MOTT 2000; Stocker, 2013) of the Dockum Group in Howard County, Texas.

It should be noted that the holotypes of *C. bryansmalli* and *T. hallae* are from approximately the same stratigraphic interval and time (Petrified Forest Member, ~212 Ma; Riggs et al., 2003; Irmis et al., 2011; Ramezani et al., 2011). This stratigraphic interval in the Chinle Formation includes more dinosaur fossils than older units, and at the Hayden Quarry, dinosaurs make up around 20% of the vertebrate assemblage (Irmis, 2008; Parker and Martz, 2011). This corresponds to a spike in species diversity in North America during the late Norian in theropods and dinosaurs in general, a trend that is sensitive to alpha taxonomy, taphonomy, and the availability of Triassic sedimentary units containing vertebrate fossils, but it is still misunderstood how it pertains to overall early dinosaur diversity (Langer et al., 2009; Irmis, 2011; Irmis et al., 2011; Ramezani et al., 2014). Our current understanding of the North American theropod fossil record suggests that the most complete specimens come from a similar stratigraphic interval, and other occurrences are far more fragmentary, which may artificially obscure actual diversity of early Theropoda throughout the Chinle Formation and into the Dockum Group.

Early Dinosaur Evolution and Missing Data

In general, it should not be surprising that *Chindesaurus bryansmalli* was not recovered in this analysis as a member of Herrerasauridae along with *Herrerasaurus ischigualastensis* and *Staurikosaurus pricei*. In fact, the first phylogenetic analysis to suggest that *C. bryansmalli* is a non-herrerasaurid, non-neotheropodan theropod is more than a decade old (Yates, 2007), albeit that analysis focused on the relationships within Sauropodomorpha. Character states formerly considered to place *C. bryansmalli* within Herrerasauridae were either not supported in a phylogenetic context (e.g., the relatively anteroposteriorly shortened trunk centra, Long and Murry, 1995; Novas, 1997; Hunt et al., 1998), are also found plesiomorphically in theropods (e.g., having two sacral vertebrae, Irmis et al., 2007; no distinct brevis fossa, Sues et al., 2011), have been improperly scored or are not possible to be unambiguously scored based on the fragmentary holotype (e.g., no groove on the dorsolateral surface of the proximal end of the ischium, Sues et al., 2011; shape of the acromion process of the scapula, Baron et al., 2017a), or are highly variable within Dinosauriformes (e.g., the presence of an anterior trochanteric shelf, Sues et al., 2011; Griffin and Nesbitt, 2016a, 2016b; Griffin, 2018; Nesbitt et al., 2018). Although variability itself is not problematic in phylogenetic analyses (for example, many tree-search algorithms account for multistate scoring), skeletally immature individuals often have different combinations of character states than mature individuals (Tykoski, 2005), and this could prove difficult in this part of the dinosaur family tree (Griffin and Nesbitt, 2016a, 2016b; Griffin, 2018; Nesbitt et al., 2018).

Two reasons for the ongoing shake-up of early dinosaur relationships (Baron et al., 2017a, 2017b; Langer et al., 2017) are the continuous introduction of new taxa and the incompleteness of the holotype fossils at the base of Dinosauria. With respect to new taxa, the discovery or reinterpretation of early members of major clades such as *Dromomeron romeri* (Lagerpetidae; Irmis et al., 2007; Nesbitt et al., 2009b), *Asilisaurus kongwe* (Silesauridae; Nesbitt et al., 2010), *Tawa hallae*, *Eodromaesus murphi*,

Daemonosaurus chauliodus, *Tachiraptor admirabilis*, and *Chilesaurus diegosuarezi* (Theropoda; Nesbitt et al., 2009c; Martinez et al., 2011; Sues et al., 2011; Langer et al., 2014; Novas et al., 2015), *Laquintasaura venezuelae* and *Pisanosaurus mertii* (Ornithischia; Barrett et al., 2014; Angolín and Rozadilla, 2017), and *Saturnalia tupiniquim* and *Eoraptor lunensis* (Sauropodomorpha; Langer, 2003; Langer et al., 2007; Martinez et al., 2011; Sereno et al., 2012) continually provides new opportunities to optimize and redistribute character states across the trees, which can turn long-standing apomorphies of major groups into plesiomorphies. Redistribution of character states with the introduction of new taxa is a strength of phylogenetic analyses and results in more meaningful biological hypotheses. One example of this is within Dinosauria; the offset (or ‘in-turned’) femoral head was a long-standing apomorphy of the group (e.g., Benton, 2004; Langer and Benton, 2006), but subsequent finds among other archosaurs suggest that this feature is found homoplastically in shuvosaurids and crocodylomorphs (Long and Murry, 1995; Nesbitt, 2007, 2011), may be present plesiomorphically in non-dinosaur dinosauromorphs (Carrano, 2000; Dzik, 2003; Ferigolo and Langer, 2007; Irmis et al., 2007; Nesbitt et al., 2009b, 2010), and probably is a complex of multiple character states with variable distribution along the archosaur tree (Langer et al., 2010; Nesbitt, 2011; Nesbitt et al., 2017).

Missing data will always be a hurdle to overcome for morphological phylogenetic analyses. However, it is important to not exclude a priori fragmentary taxa such as *C. bryansmalli* from an analysis (even though it is rarely scored for more than 20% of the characters in a given analysis; Table 1), because total-evidence approaches can result in more robust phylogenetic hypotheses (Gauthier et al., 1988; Donoghue et al., 1989; Kluge, 1989, 1998). Taxa with missing data may be useful in breaking up long branches and in reconstructing ancestral character states (Wiens, 2003), but this may not always be the case. Such taxa can also act as ‘wildcards,’ however, appearing in disparate parts of the tree with the addition or removal of important character-state changes or taxa (Donoghue et al., 1989; Norell and Wheeler, 2003; Kearney, 2002; Kearney and Clark, 2003). Even though Bremer support for the ‘traditional’ hypothesis of dinosaur relationships is fairly high for some major lineages in our analysis (6 for Dinosauria, 5 for Ornithischia, 6 for Saurischia, and 6 for Theropoda), it is low for others (1 for Sauropodomorpha), and the data set lacks important ingroup members of those lineages that would help optimize character-state distribution, such as marginocephalians, ornithopods, and sauropods. The limitation of this data set in resolving certain ingroup relationships is exemplified by the polytomy at Tetanurae (Fig. 10). This lack of resolution and support also may be from conflicting phylogenetic signal across disparate anatomical modules in the skeleton owing to mosaic evolution, which should be tested in future studies (Parker, 2016).

It is extremely important when designing a study that researchers establish the most suitable data set for the question in mind, rather than designing a question suitable to a preexisting data matrix. It can be time-saving to use an existing matrix that roughly parallels a research question, but it is not true that a given matrix can be used to answer questions other than those for which it was first constructed. Using a poorly suited matrix can introduce parsimony-uninformative characters that can contribute character conflict to the analysis (Nixon and Carpenter, 1993; Milinkovitch and Lyons-Weiler, 1998; Luo et al., 2010). Systematists need to be intentional when selecting a data matrix; the best practice is to either construct or choose one (or more) suitable data set(s) with a specific question in mind and to document every decision made regarding character description, outgroup and ingroup OTU choice, and scoring. It is this documentation that makes a phylogenetic analysis rigorous, not necessarily the

support values for the topological nodes or other measures of tree support.

Matrices originally built for the same purpose evolve over time and the phylogenetic hypotheses derived from them can vary considerably. The Yates (2007) and Upchurch et al. (2007) matrices were both built to hypothesize ingroup relationships among non-sauropod sauropodomorphs (or ‘basal sauropodomorphs’). One recovered basal sauropodomorphs as a paraphyletic grade of organisms between *Saturnalia tupiniquim* and Sauropoda (Yates, 2007), whereas the other found a monophyletic Prosauropoda as the sister taxon to Sauropoda (Upchurch et al., 2007). Subsequently, it has been common for new specimens of basal sauropodomorphs to be included in modified versions of both analyses (e.g., Sertich and Loewen, 2010; Rowe et al., 2011; Apaldetti et al., 2013; Marsh and Rowe, 2018), often with widely different results (de Fabr egues et al., 2015). If tree topologies vary between two different data sets, it is difficult to determine which of the two hypotheses is ‘better’ than the other one. Phylogenetic systematics is an inherently iterative process, and it is important to remember that the outcomes of such analyses (trees constructed using parsimony, likelihood, or Bayesian statistics) are hypotheses and that hypotheses are meant to be repeatedly tested (Wiley, 1975; Gaffney, 1979).

CONCLUSIONS

Our study contributes to a better understanding of the anatomy of the holotype of *Chindesaurus bryansmalli*, and the novel characters and scoring changes provided here should be incorporated in future analyses that include this taxon. Even though *C. bryansmalli* is at best scored for 26% of the characters in a phylogenetic analysis, it is well supported as the sister taxon to *Tawa hallae* just outside of Neotheropoda. Its unique suite of anatomical characters, along with its geographic and stratigraphic range, makes *C. bryansmalli* an important taxon in reconstructing the early evolutionary history of theropod dinosaurs, especially in North America. We suggest that despite historic and ongoing changes to the dinosaur family tree, the phylogenetic hypotheses of stem-averostran theropods may become increasingly stable, even with the inclusion of fragmentary taxa.

ACKNOWLEDGMENTS

We thank the Laborat orio de Paleontologia at the Universidade de S o Paulo, Ribeir o Preto, the Jackson School of Geosciences at the University of Texas at Austin, and the Petrified Forest Museum Association for funding this work and the Congreso Latinoamericano de Paleontologia for the invitation to present our research at the fifth conference in Colonia del Sacramento, Uruguay. We thank T. Rowe, C. Bell, J. Clarke, D. Stockli, and H.-D. Sues for reviewing an early draft of the manuscript. M. Smith (PEFO), P. Holroyd, K. Padian, and M. Goodwin (UCMP), B. Sanders (UMMP), A. Downs (GR), and C. Sagebiel and M. Brown (TMM) provided access to specimens. We especially thank R. Long and T. Rowe for discussions on the excavation and preparation of the holotype of *Chindesaurus bryansmalli*. We thank T. Rowe, L. Gordon, H. Hutchison, N. Simmons, K. Ballew, B. Small, and the late M. Greenwald for collecting the holotype specimen. R. Long’s field notes are on file in the PEFO museum archives. We thank M. Bronzati and J. Marsola for helpful comparative photographs. Reviews by R. Butler and M. Ezcurra enhanced the manuscript. This is Petrified Forest National Park Contribution No. 63. The conclusions presented here are those of the authors and do not represent the views of the United States Government.

ORCID

Adam D. Marsh  <http://orcid.org/0000-0002-3223-8940>
 William G. Parker  <http://orcid.org/0000-0002-6005-7098>
 Max C. Langer  <http://orcid.org/0000-0003-1009-4605>
 Sterling J. Nesbitt  <http://orcid.org/0000-0002-7017-1652>

LITERATURE CITED

- Agnolín, F. L., and S. Rozadilla. 2017. Phylogenetic reassessment of *Pisanosaurus mertii* Casamiquela, 1967, a basal dinosauriform from the Late Triassic of Argentina. *Journal of Systematic Palaeontology* 16:853–879.
- Apaldetti, C., D. Pol, and A. Yates. 2013. The postcranial anatomy of *Coloradisaurus brevis* (Dinosauria: Sauropodomorpha) from the Late Triassic of Argentina and its phylogenetic implications. *Palaeontology* 56:1–25.
- Baron, M. G., and P. M. Barrett. 2017. A dinosaur missing-link? *Chilesaurus* and the early evolution of ornithischian dinosaurs. *Biology Letters* 13:20170220.
- Baron, M. G., and M. E. Williams. 2018. A re-evaluation of the enigmatic dinosauriform *Caseosaurus crosbyensis* from the Late Triassic of Texas, USA and its implications for early dinosaur evolution. *Acta Palaeontologica Polonica* 63:129–145.
- Baron, M. G., D. B. Norman, and P. M. Barrett. 2017a. A new hypothesis of dinosaur relationships and early dinosaur evolution. *Nature* 543:501–506.
- Baron, M. G., D. B. Norman, and P. M. Barrett. 2017b. Baron et al. reply. *Nature* 551:E4–E5. doi: 10.1038/nature24012.
- Baron, M. G., D. B. Norman, and P. M. Barrett. 2017c. Postcranial anatomy of *Lesothosaurus diagnosticus* (Dinosauria: Ornithischia) from the Lower Jurassic of southern Africa: implications for basal ornithischian taxonomy and systematics. *Zoological Journal of the Linnean Society* 179:125–168.
- Barrett, P. M., R. J. Butler, R. Mundil, T. M. Scheyer, R. B. Irmis, and M. R. Sánchez-Villagra. 2014. A paleoequatorial ornithischian and new constraints on early dinosaur diversification. *Proceedings of the Royal Society B: Biological Sciences* 281:20141147. doi: 10.1098/rspb.2014.1147.
- Benton, M. J. 2004. Origin and relationships of Dinosauria; pp. 7–19 in D. B. Weishampel, P. Dodson, and H. Osmólska (eds.), *The Dinosauria*, second edition. University of California Press, Berkeley, California.
- Bittencourt, J. S., and A. W. A. Kellner. 2009. The anatomy and phylogenetic position of the Triassic dinosaur *Staurikosaurus pricei* Colbert, 1970. *Zootaxa* 2079:1–56.
- Bonaparte, J. F. 1986. Les Dinosauriens (Carnosauriens, Allosauridés, Sauropodes, Cétiosauridés) du Jurassique Moyen de Cerro Condor (Chubut, Argentine). *Annales de Paléontologie (Vert.-Invert.)* 72:325–386.
- Bonaparte, J. F., J. Ferigolo, and A. M. Ribeiro. 1999. A new early Late Triassic saurischian dinosaur from Rio Grande do Sul state, Brazil. *National Science Museum Monographs* 15:89–109.
- Bonaparte, J. F., G. Brea, L. Schultz, and A. G. Martinelli. 2007. A new specimen of *Guaibasaurus candelariensis* (basal Saurischia) from the Late Triassic Caturrita Formation of southern Brazil. *Historical Biology* 19:73–82.
- Brochu, C. A. 1996. Closure of neurocentral sutures during crocodylian ontogeny: implications for maturity assessment in fossil archosaurs. *Journal of Vertebrate Paleontology* 16:49–62.
- Cabreira, S. F., A. W. A. Kellner, S. Dias-da-Silva, L. R. da Silva, M. Bronzati, J. C. A. Marsola, R. T. Müller, J. S. Bittencourt, B. J. Batista, T. Raugust, R. Carrilho, A. Brodt, and M. C. Langer. 2016. A unique Late Triassic dinosauriform assemblage reveals dinosaur ancestral anatomy and diet. *Current Biology* 26:3090–3095.
- Carrano, M. T. 2000. Homoplasy and the evolution of dinosaur locomotion. *Paleobiology* 26:489–512.
- Case, E. C. 1927. The vertebral column of *Coelophysis* Cope. *Contributions from the Museum of Geology, University of Michigan* 2:209–222.
- Clark, J. M., H.-D. Sues, and D. S. Berman. 2000. A new specimen of *Hesperosuchus agilis* from the Upper Triassic of New Mexico and the interrelationships of basal crocodylomorph archosaurs. *Journal of Vertebrate Paleontology* 20:683–704.
- Colbert, E. H. 1952. A pseudosuchian reptile from Arizona. *Bulletin of the American Museum of Natural History* 99:561–592.
- Colbert, E. H. 1981. A primitive ornithischian dinosaur from the Kayenta Formation of Arizona. *Museum of Northern Arizona Bulletin* 53:1–61.
- Colbert, E. H. 1989. The Triassic dinosaur *Coelophysis*. *Museum of Northern Arizona Bulletin* 57:1–160.
- Colbert, E. H. 1990. Variation in *Coelophysis bauri*; pp. 81–90 in K. Carpenter and P. J. Currie (eds.), *Dinosaur Systematics: Perspectives and Approaches*. Cambridge University Press, Cambridge, U.K.
- Donoghue, M. J., J. A. Doyle, J. Gauthier, A. G. Kluge, and T. Rowe. 1989. The importance of fossils in phylogeny reconstruction. *Annual Review of Ecology and Systematics* 20:431–460.
- Dunbar, L., and C. Robson. 1986. A Whopping Small Dinosaur. Harbringer Films, Coronet Film and Video, Northbrook, Illinois.
- Dzik, J. 2003. A beaked herbivorous archosaur with dinosaur affinities from the early Late Triassic Period of Poland. *Journal of Vertebrate Paleontology* 23:556–574.
- Evans, E. L., Griffin, C. T., Smith, N., Turner, A. H., Irmis, R. B., and S. J. Nesbitt. 2018. Ontogenetic changes in the femur of *Tawa hallae* and implications for species diversity of Late Triassic dinosaurs. *Journal of Vertebrate Paleontology* 38(Program and Abstracts):123.
- Ezcurra, M. D., and S. L. Brusatte. 2011. Taxonomic and phylogenetic reassessment of the early neotheropod dinosaur *Camposaurus arizonensis* from the Late Triassic of North America. *Palaeontology* 54:763–772.
- Fabrégues, C. P. de, R. Allain, and V. Barriel. 2015. Root cause of phylogenetic incongruence observed within basal sauropodomorph interrelationships. *Zoological Journal of the Linnean Society* 175:569–586.
- Ferigolo, J., and M. C. Langer. 2007. A Late Triassic dinosauriform from south Brazil and the origin of the ornithischian predecestry bone. *Historical Biology* 19:23–33.
- Gaffney, E. S. 1979. An introduction to the logic of phylogeny reconstruction; pp. 79–111 in J. Cracraft and N. Eldredge (eds.), *Phylogenetic Analysis and Paleontology*. Columbia University Press, New York.
- Galton, P. M. 1977. On *Staurikosaurus pricei*, an early saurischian dinosaur from the Triassic of Brazil, with notes on the Herrerasauridae and Poposauridae. *Paläontologische Zeitschrift* 51:234–245.
- Gauthier, J., A. G. Kluge, and T. Rowe. 1988. Amniote phylogeny and the importance of fossils. *Cladistics* 4:105–209.
- Goloboff, P., J. Farris, and K. Nixon. 2008. TNT: a free program for phylogenetic analysis. *Cladistics* 24:774–786.
- Griffin, C. T. 2018. Developmental patterns and variation among early theropods. *Journal of Anatomy* 232:604–640.
- Griffin, C. T., and S. J. Nesbitt. 2016a. The femoral ontogeny and long bone histology of the Middle Triassic (?late Anisian) dinosauriform *Asilisaurus kongwe* and implications for the growth of early dinosaurs. *Journal of Vertebrate Paleontology*. doi: 10.1080/02724634.2016.1111224.
- Griffin, C. T., and S. J. Nesbitt. 2016b. Anomalous high variation in post-natal development is ancestral for dinosaurs but lost in birds. *Proceedings of the National Academy of Sciences of the United States of America* 113:14757–14762.
- Heckert, A. B., S. G. Lucas, and R. M. Sullivan. 2000. Triassic dinosaurs in New Mexico; pp. 17–26 in S. G. Lucas and A. B. Heckert (eds.), *Dinosaurs of New Mexico*. New Mexico Museum of Natural History and Science Bulletin 17. Albuquerque, New Mexico.
- Huene, F. R. von. 1934. Ein neuer Coelurosaurier in der thüringischen Trias. *Palaeontologische Zeitschrift* 16:145–170.
- Hunt, A. P., S. G. Lucas, A. B. Heckert, R. M. Sullivan, and M. G. Lockley. 1998. Late Triassic dinosaurs from the western United States. *Geobios* 31:511–531.
- Irmis, R. B. 2007. Axial skeleton ontogeny in the Parasuchia (Archosauria: Pseudosuchia) and its implications for ontogenetic determination in archosaurs. *Journal of Vertebrate Paleontology* 27:350–361.
- Irmis, R. B. 2008. Perspectives on the origin and early diversification of dinosaurs. Ph.D. dissertation, University of California, Berkeley, California, 421 pp.
- Irmis, R. B. 2011. Evaluating hypotheses for the early diversification of dinosaurs. *Earth and Environmental Science Transactions of the Royal Society of Edinburgh* 101:397–426.
- Irmis, R. B., R. Mundil, J. W. Martz, and W. G. Parker. 2011. High-resolution U-Pb ages from the Upper Triassic Chinle Formation (New Mexico, USA) support a diachronous rise of dinosaurs. *Earth and Planetary Science Letters* 309:258–267.

- Irmis, R. B., S. J. Nesbitt, K. Padian, N. D. Smith, A. H. Turner, D. Woody, and A. Downs. 2007. A Late Triassic dinosauriform assemblage from New Mexico and the rise of dinosaurs. *Science* 317:358–361.
- Kearney, M. 2002. Fragmentary taxa, missing data, and ambiguity: mistaken assumptions and conclusions. *Systematic Biology* 51:369–381.
- Kearney, M., and J. M. Clark. 2003. Problems due to missing data in phylogenetic analyses including fossils: a critical review. *Journal of Vertebrate Paleontology* 23:263–274.
- Kluge, A. G. 1989. A concern for evidence and a phylogenetic hypothesis of relationships among *Epicrates* (Boidae, Serpentes). *Systematic Zoology* 38:7–25.
- Kluge, A. G. 1998. Total evidence or taxonomic congruence: cladistics or consensus classification. *Cladistics* 14:151–158.
- Langer, M. C. 2003. The pelvic and hind limb anatomy of the stem-sauropodomorph *Saturnalia tupiniquim* (Late Triassic, Brazil). *PaleoBios* 23:1–30.
- Langer, M. C. 2004. Basal Saurischia; pp. 25–46 in D. B. Weishampel, P. Dodson, and H. Osmólska (eds.), *The Dinosauria*, second edition. University of California Press, Berkeley, California.
- Langer, M. C., and M. J. Benton. 2006. Early dinosaurs: a phylogenetic study. *Journal of Systematic Palaeontology* 4:309–358.
- Langer, M. C., and J. S. Bittencourt. 2014. New developments into early dinosaur phylogeny; p. 559 in 4th International Palaeontological Congress, September 28–October 3, 2014, Mendoza, Argentina. Compiled by Cerdeño, E. Published by the International Palaeontological Association.
- Langer, M. C., M. D. Ezcurra, J. S. Bittencourt, and F. E. Novas. 2010. The origin and early evolution of dinosaurs. *Biological Reviews* 85:55–110. doi:10.1111/j.1469-185X.2009.00094.x
- Langer, M. C., J. S. Bittencourt, and C. L. Schultz. 2011. A reassessment of the basal dinosaur *Guaibasaurus candelariensis*, from the Late Triassic Caturrita Formation of South Brazil. *Earth and Environmental Science Transactions of the Royal Society of Edinburgh* 101:301–332.
- Langer, M. C., M. A. G. Franca, and S. Gabriel. 2007. The pectoral girdle and forelimb anatomy of the stem-sauropodomorph *Saturnalia tupiniquim* (Upper Triassic, Brazil). *Special Papers in Palaeontology* 77:113–137.
- Langer, M. C., A. G. Martinelli, and A. D. Marsh. 2016. New data on *Guaibasaurus candelariensis*, a saurischian dinosaur from the Norian of Brazil; p. 30 in *Jornadas Argentinas de Paleontología de Vertebrados*; May 17–20, 2016, Buenos Aires, Argentina, (Museo Argentino de Ciencias Naturales), no editors. This abstract is also published in *Ameghiniana* 53(6):60.
- Langer, M. C., F. Abdala, M. Richter, and M. J. Benton. 1999. A sauropodomorph dinosaur from the Upper Triassic (Carnian) of southern Brazil. *Comptes Rendus de l'Académie des Sciences, Series IIA, Earth and Planetary Science* 329:511–517.
- Langer, M. C., M. D. Ezcurra, J. S. Bittencourt, and F. E. Novas. 2009. The origin and early evolution of dinosaurs. *Biological Reviews* 85:1–56.
- Langer, M. C., A. D. Rincón, J. Ramezani, A. Solórzano, and O. W. M. Rauhut. 2014. New dinosaur (Theropoda, stem-Averostra) from the earliest Jurassic of the La Quinta formation, Veneuelan Andes. *Royal Society Open Science* 1:140184. doi: 10.1098/rsos.140184.
- Langer, M. C., M. D. Ezcurra, O. W. M. Rauhut, M. K. Benton, F. Knoll, B. W. McPhee, F. E. Novas, D. Pol, and S. L. Brusatte. 2017. Untangling the dinosaur family tree. *Nature* 551:E1–E3. doi: 10.1038/nature24011.
- Long, R. A., and P. A. Murry. 1995. Late Triassic (Carnian and Norian) tetrapods from the Southwestern United States. *New Mexico Museum of Natural History and Science Bulletin* 4:1–254.
- Luo, A. R., Y. Zhang, H. Qiao, W. Shi, R. W. Murphy, and C. Zhu. 2010. Outgroup selection in tree reconstruction: a case study of the family Halictidae (Hymenoptera: Apoidea). *Acta Entomologica Sinica* 53:192–201.
- Maddison, W. P., and D. R. Maddison. 2015. Mesquite: a modular system for evolutionary analysis, version 3.04. Available at mesquitemproject.org. Accessed September 24, 2016.
- Marsh, A. D., and T. B. Rowe. 2018. Anatomy and systematics of the sauropodomorph *Sarhsaurus aurifontanalis* from the Early Jurassic Kayenta Formation. *PLoS ONE* 13:e0204007.
- Marsh, O. C. 1881. Principal characters of American Jurassic dinosaurs. *American Journal of Science* 3:417–423.
- Martinez, R. N., P. C. Sereno, O. A. Alcobar, C. E. Colombi, P. R. Renne, I. P. Montañez, and B. S. Currie. 2011. A basal dinosaur from the dawn of the dinosaurs era in southwestern Pangaea. *Science* 331:206–210.
- Martz, J. W., and W. G. Parker. 2010. Revised lithostratigraphy of the Sonsela Member (Chinle Formation, Upper Triassic) in the southern part of Petrified Forest National Park, Arizona. *PLoS ONE* 5:e9329.
- Martz, J. W., W. G. Parker, L. Skinner, J. J. Raucci, P. Umhoefer, and R. C. Blakey. 2012. Geologic map of Petrified Forest National Park, Arizona. Arizona Geological Survey Contributed Map CR-12-A, 1 map sheet, 1:50,000 map scale.
- Meyer, L. L. 1986. D-Day in the Painted Desert; pp. 2–13 in M. Windsor (ed.), *Arizona Highways*, June 1986, 62(7), Phoenix, Arizona. Published by the Arizona Department of Transportation, Phoenix, AZ.
- Milinkovitch, M. C., and J. Lyons-Weiler. 1998. Finding optimal ingroup topologies and convexities when the choice of outgroups is not obvious. *Molecular Phylogenetics and Evolution* 9:348–357.
- Miller, J. A. 1985. Ghost from the dawn of the dinosaurs. *Science News* 127:325.
- Morris, Z. M., and S. Werning. 2012. Histological variation suggests unusual levels of developmental plasticity in the stem archosaur *Vancleavea*. *Journal of Vertebrate Paleontology* 32(Program and Abstracts):146.
- Murry, P. A., and R. A. Long. 1989. Geology and paleontology of the Chinle Formation, Petrified Forest National Park and vicinity, Arizona and a discussion of vertebrate fossils of the southwestern Upper Triassic; pp. 29–64 in S. G. Lucas and A. P. Hunt (eds.), *Dawn of the Age of Dinosaurs in the American Southwest*. New Mexico Museum of Natural History and Science, Albuquerque, New Mexico.
- Nesbitt, S. J. 2007. The anatomy of *Effigia okeeffeae* (Archosauria, Suchia), theropod convergence, and the distribution of related taxa. *Bulletin of the American Museum of Natural History* 302:1–84.
- Nesbitt, S. J. 2011. The early evolution of archosaurs: relationships and the origin of major clades. *Bulletin of the American Museum of Natural History* 352:1–292.
- Nesbitt, S. J., and S. Chatterjee. 2008. Late Triassic dinosauriforms from the Post Quarry and surrounding areas, west Texas, USA. *Neues Jahrbuch für Geologie und Paläontologie, Abhandlungen* 249:143–156.
- Nesbitt, S. J., and M. D. Ezcurra. 2015. The early fossil record of dinosaurs in North America: a new neotheropod from the base of the Upper Triassic Dockum Group of Texas. *Acta Palaeontologica Polonica* 60:513–526.
- Nesbitt, S. J., R. B. Irmis, and W. G. Parker. 2007. A critical re-evaluation of the Late Triassic dinosaur taxa of North America. *Journal of Systematic Paleontology* 5:209–243.
- Nesbitt, S. J., M. R. Stocker, B. J. Small, and A. Downs. 2009a. The osteology and relationships of *Vancleavea campi* (Reptilia: Archosauriformes). *Zoological Journal of the Linnean Society* 157:814–864.
- Nesbitt, S. J., R. B. Irmis, W. G. Parker, N. D. Smith, A. H. Turner, and T. Rowe. 2009b. Hindlimb osteology and distribution of basal dinosauriforms from the Late Triassic of North America. *Journal of Vertebrate Paleontology* 29:498–516.
- Nesbitt, S. J., C. A. Sidor, R. B. Irmis, K. D. Angielczyk, R. M. Smith, and L. A. Tsuji. 2010. Ecologically distinct dinosaurian sister group shows early diversification of Ornithodira. *Nature* 464:95–98.
- Nesbitt, S. J., N. D. Smith, R. B. Irmis, A. H. Turner, A. Downs, and M. A. Norell. 2009c. A complete skeleton of a Late Triassic saurischian and the early evolution of dinosaurs. *Science* 326:1530–1533.
- Nesbitt, S. J., C. Griffin, E. Evans, R. T. Mueller, C. Pacheco, F. Preto, S. Cabreira, A. D. Marsh, B. M. Wynd, and M. C. Langer. 2018. Prevalent ontogenetic changes characterize early dinosaurs and their closest relatives: implications for species identification, phylogeny, and the loss of these changes in later dinosaurs. *Journal of Vertebrate Paleontology* 38(Program and Abstracts):190.
- Nesbitt, S. J., R. J. Butler, M. D. Ezcurra, P. M. Barrett, M. R. Stocker, K. D. Angielczyk, R. M. H. Smith, C. A. Sidor, G. Niedzwiedzki, A. G. Sennikov, and A. J. Charig. 2017. The earliest bird-line archosaurs and the assembly of the dinosaur body plan. *Nature* 544:484–487.
- Nixon, K. C., and J. M. Carpenter. 1993. On outgroups. *Cladistics* 9:413–426.
- Norell, M. A., and W. Wheeler. 2003. Missing entry replacement data analysis: a replacement approach to dealing with missing data in paleontological and total evidence data sets. *Journal of Vertebrate Paleontology* 23:275–283.
- Novas, F. E. 1993. New information on the systematics and postcranial skeleton of *Herrerasaurus ischigualastensis* (Theropoda: Herrerasauridae) from the Ischigualasto Formation (Upper Triassic) of Argentina. *Journal of Vertebrate Paleontology* 13:400–423.

- Novas, F. E. 1997. Herrerasauridae; pp. 303–311 in P. J. Currie and K. Padian (eds.), *Encyclopedia of Dinosaurs*. Academic Press, San Diego, California.
- Novas, F. E., S. L. Suárez, F. L. Angolín, M. N. Ezcurra, N. S. R. Chimento, R. de la Cruz, M. P. Isasi, A. O. Vargas, and D. Rubilar-Rogers. 2015. An enigmatic plant-eating theropod from the Late Jurassic period of Chile. *Nature* 522:331–334.
- Owen, R. 1842. Report on British fossil reptiles, part II. Report of the British Association of the Advancement of Science 11:60–104.
- Padian, K. 1988. New discoveries about dinosaurs: separating the facts from the news. *Journal of Geological Education* 36:215–220.
- Padian, K. 2013. Why study the bone microstructure of fossil tetrapods?; pp. 1–12 in K. Padian and E.-T. Lamm (eds.), *Bone Histology of Fossil Tetrapods*. University of California Press, Berkeley, California.
- Parker, W. G. 2002. Correlation of locality numbers for fossil vertebrate sites in Petrified Forest National Park, Arizona; pp. 37–42 in A. B. Heckert and S. G. Lucas (eds.), *Upper Triassic Stratigraphy and Paleontology*. New Mexico Museum of Natural History and Science Bulletin 21. Albuquerque, New Mexico.
- Parker, W. G. 2006. The stratigraphic distribution of major fossil localities in Petrified Forest National Park; pp. 46–61 in W. G. Parker, S. R. Ash, and R. B. Irmis (eds.), *A Century of Research at Petrified Forest National Park*. Museum of Northern Arizona Bulletin 62. Flagstaff, Arizona.
- Parker, W. G. 2016. Revised phylogenetic analysis of the Aetosauria (Archosauria: Pseudosuchia); assessing the effects of incongruent morphological character sets. *PeerJ* 4:e1583.
- Parker, W. G., and B. J. Barton. 2008. New information on the Upper Triassic archosauriform *Vancleavea campi* based on new material from the Chinle Formation of Arizona. *Palaeontologia Electronica* volume 11, issue 3, article 14A. https://www.uv.es/~pardomv/pe/2008_3/158/index.html.
- Parker, W. G., and R. B. Irmis. 2005. Advances in Late Triassic vertebrate paleontology based on new material from Petrified Forest National Park, Arizona; pp. 45–58 in A. B. Heckert and S. G. Lucas (eds.), *Vertebrate Paleontology in Arizona*. New Mexico Museum of Natural History and Science Bulletin 29. Albuquerque, New Mexico.
- Parker, W. G., and J. W. Martz. 2011. The Late Triassic (Norian) Adamanian-Revueletian tetrapod faunal transition in the Chinle Formation of Petrified Forest National Park, Arizona. *Earth and Environmental Science Transactions of the Royal Society of Edinburgh* 101:231–260.
- Parrish, J. M. 1991. A new specimen of an early crocodylomorph (cf. *Sphenosuchus* sp.) from the Upper Triassic Chinle Formation of Petrified Forest National Park, Arizona. *Journal of Vertebrate Paleontology* 11:198–212.
- Piechowski, R., and J. Dzik. 2010. The axial skeleton of *Silesaurus opolenensis*. *Journal of Vertebrate Paleontology* 30:1127–1141.
- Ramezani, J., D. E. Fastovsky, and S. A. Bowring. 2014. Revised chronostratigraphy of the lower Chinle Formation strata in Arizona and New Mexico (USA): high-precision U-Pb geochronological constraints on the Late Triassic evolution of dinosaurs. *American Journal of Science* 314:981–1008.
- Ramezani, J., G. D. Hoke, D. E. Fastovsky, S. A. Bowring, F. Therrien, S. T. Dworkin, S. C. Atchley, and L. C. Nordt. 2011. High-precision U-Pb zircon geochronology of the Late Triassic Chinle Formation, Petrified Forest National Park (Arizona, USA): temporal constraints on the early evolution of dinosaurs. *Geological Society of America Bulletin* 123:2142–2159.
- Rauhut, O. W. M. 2003. The interrelationships and evolution of basal theropod dinosaurs. *Special Papers in Palaeontology* 69:1–213.
- Riggs, N. R., S. R. Ash, A. P. Barth, G. E. Gehrels, and J. L. Wooden. 2003. Isotopic age of the Black Forest Bed, Petrified Forest Member, Chinle Formation, Arizona: an example of dating a continental sandstone. *Geological Society of America Bulletin* 115:1315–1323.
- Rowe, T. 1989. A new species of the theropod dinosaur *Syntarsus* from the Early Jurassic Kayenta Formation of Arizona. *Journal of Vertebrate Paleontology* 9:125–136.
- Rowe, T. B., H.-D. Sues, and R. R. Reisz. 2011. Dispersal and diversity in the earliest North American sauropodomorph dinosaurs, with a description of a new taxon. *Proceedings of the Royal Society of London B: Biological Sciences* 278:1044–1053.
- Sarigül, V. 2017. New theropod fossils from the Upper Triassic Dockum Group of Texas, USA, and a brief overview of the Dockum theropod diversity. *PaleoBios* 34:1–18.
- Seeley, H. G. 1887. On the classification of the fossil animals commonly named Dinosauria. *Proceedings of the Royal Society of London* 43:165–171.
- Sereno, P. C. 1999. The evolution of dinosaurs. *Science* 284:2137–2147.
- Sereno, P. C. 2005. The logical basis of phylogenetic taxonomy. *Systematic Biology* 54:595–619.
- Sereno, P. C., and F. E. Novas. 1994. The skull and neck of the basal theropod *Herrerasaurus ischigualastensis*. *Journal of Vertebrate Paleontology* 13:451–476.
- Sereno, P. C., R. N. Martínez, and O. A. Alcobar. 2012. Osteology of *Eoraptor lunensis* (Dinosauria, Sauropodomorpha); pp. 83–179 in P. C. Sereno (ed.), *Basal Sauropodomorphs and the Vertebrate Fossil Record of the Ischigualasto Formation (Late Triassic: Carnian-Norian) of Argentina*. Society of Vertebrate Paleontology Memoir 12. *Journal of Vertebrate Paleontology* 32(Supplement 1).
- Sertich, J. J. W., and M. A. Loewen. 2010. A new basal sauropodomorph dinosaur from the Lower Jurassic Navajo Sandstone of southern Utah. *PLoS ONE* 5:e9789.
- Smith, N. D., P. J. Makovicky, W. R. Hammer, and P. J. Currie. 2007. Osteology of *Cryolophosaurus ellioti* (Dinosauria: Theropoda) from the Early Jurassic of Antarctica and implications for early theropod evolution. *Zoological Journal of the Linnean Society* 151:377–421.
- Stocker, M. R. 2013. Contextualizing vertebrate faunal dynamics: new perspectives from the Triassic and Eocene of western North America. Ph.D. dissertation, University of Texas at Austin, Austin, Texas, 297 pp.
- Sues, H.-D., S. J. Nesbitt, D. S. Berman, and A. C. Henrici. 2011. A late-surviving basal theropod dinosaur from the latest Triassic of North America. *Proceedings of the Royal Society of London B: Biological Sciences* 278:rsrb20110410. doi: 10.1098/rsrb.2011.0410.
- Tykoski, R. S. 1998. The osteology of *Syntarsus kayentakatae* and its implications for ceratosaurid phylogeny. M.Sc. thesis, University of Texas at Austin, Austin, Texas, 217 pp.
- Tykoski, R. S. 2005. Anatomy, ontogeny, and phylogeny of coelophysoid theropods. Ph.D. dissertation, University of Texas at Austin, Austin, Texas, 553 pp.
- Yates, A. M. 2007. The first complete skull of the Triassic dinosaur *Melanorosaurus* Houghton (Sauropodomorpha: Anchisauria); pp. 9–55 in P. M. Barrett and D. J. Batten (eds.), *Evolution and Palaeobiology of Early Sauropodomorph Dinosaurs*. *Special Papers in Palaeontology* 77. The Palaeontological Association, London, U.K.
- Upchurch, P., P. M. Barrett, and P. M. Galton. 2007. A phylogenetic analysis of basal sauropodomorph relationships: implications for the origin of sauropod dinosaurs; pp. 57–90 in P. M. Barrett and D. J. Batten (eds.), *Evolution and Palaeobiology of Early Sauropodomorph Dinosaurs*. *Special Papers in Palaeontology* 77. The Palaeontological Association, London, U.K.
- Walker, A. D. 1970. A revision of the Jurassic reptile *Hallopus victor* (Marsh), with remarks on the classification of crocodiles. *Philosophical Transactions of the Royal Society of London B: Biological Sciences* 257:323–372.
- Welles, S. P. 1984. *Dilophosaurus wetherilli* (Dinosauria, Theropoda): osteology and comparisons. *Palaeontographica Abteilung A* 185:84–180.
- Wiens, J. J. 2003. Missing data, incomplete taxa, and phylogenetic accuracy: is there a missing data problem? *Systematic Biology* 52:528–538.
- Wiley, E. O. 1975. Karl R. Popper, systematics, and classification: a reply to Walter Bock and other evolutionary systematists. *Systematic Zoology* 24:233–243.
- Wilson, J. A. 1999. A nomenclature for vertebral laminae in sauropods and other saurischian dinosaurs. *Journal of Vertebrate Paleontology* 19:639–653.
- Wilson, J. A., M. D. D’Emic, T. Ikejiri, E. M. Moacdieh, and J. A. Whitlock. 2011. A nomenclature for vertebral fossae in sauropods and other saurischian dinosaurs. *PLoS ONE* 6:e17114.
- Wilson, J. A., D. C. Woodruff, J. D. Gardner, H. M. Flora, J. R. Horner, and C. L. Organ. 2016. Vertebral adaptations to large body size in theropod dinosaurs. *PLoS ONE* 11:e0158962.
- Woodward, H. N., K. Padian, and A. H. Lee. 2013. Skeletochronology; pp. 195–215 in K. Padian and E.-T. Lamm (eds.), *Bone Histology of Fossil Tetrapods*. University of California Press, Berkeley, California.

Submitted February 16, 2019; revisions received May 27, 2019;

accepted June 5, 2019.

Handling editor: Elizabeth Martin-Silverstone.